KFKI-1981-79

L. KOBLINGER

POKER-CAMP: A PROGRAM FOR CALCULATING DETECTOR RESPONSES AND PHANTOM ORGAN DOSES IN ENVIRONMENTAL GAMMA FIELDS

Hungarian Academy of Sciences

CENTRAL
RESEARCH
INSTITUTE FOR
PHYSICS

BUDAPEST

KFKI-1981-79

POKER-CAMP: A PROGRAM FOR CALCULATING DETECTOR RESPONSES AND PHANTOM ORGAN DOSES IN ENVIRONMENTAL GAMMA FIELDS

László Koblinger

Central Research Institute for Physics
H-1525 Budapest 114, P.O.B.49, Hungary

HU ISSN 0368 5330
ISBN 963 371 861 9

ABSTRACT

A general description, user's manual and a sample problem are given in this report on the POKER-CAMP adjoint Monte Carlo photon transport program.

Gamma fields of different environmental sources which are uniformly or exponentially distributed sources or plane sources in the air, in the soil or in an intermediate layer placed between them are simulated in the code.

Calculations can be made on flux, kerma and spectra of photons at any point; and on responses of point-like, cylindrical, or spherical detectors; and on doses absorbed in anthropomorphic phantoms.

АННОТАЦИЯ

В статье дается ознакомление с адаптированной для расчета транспорта фотонов методом Monte-Carlo программой, названной POKER-CAMP. Общее руководство по применению программы дополнено необходимой информацией и примером применения программы.

С помощью программы можно моделировать поля излучения, происходящие от различных гамма-источников окружающей среды. Источники могут быть размещены в трех средах: в воздухе, в почве и каком-нибудь промежуточном слое с равномерным или экспоненциальным распределением, а также разложенными в плоском слое.

С помощью программы имеется возможность рассчитать в любой произвольной точке измеряемый поток и воздушную керму, а также спектр проходящих через данную точку фотонов; сигнализацию различных детекторов или поглощенные дозы органами антропоморфного фантома, поставленного на почву.

KIVONAT

Reportunkban a POKER-CAMP nevü adjungált Monte Carlo foton transzport programot ismertetjük. Az általános leirást a program felhasználásához szükséges információk és egy minta feladat egészíti ki.

A programmal különböző környezeti gamma forrásoktól eredő sugárzás-terek modellezhetők. Három régióba: a levegőbe, a talajba és egy közbülső rétegbe helyezhetők el térben egyenletesen, vagy exponenciálisan elosztott, illetve sik rétegben szétteritett források.

A program egy tetszőleges pontban mérhető fluxust és levegő-kermát és a ponton áthaladó fotonok spektrumát; különböző detektorok jelzését; vagy a talajra állitott antropomorf fantomok szerveiben elnyelt dózisokat számolja.

C O N T E N T S

1. INTRODUCTION

The aim of the work described here was to construct a computer code that can be used for calculating detector responses and human doses in environmental gamma fields. The gamma emitters can be natural sources, or those originating, for example, from nuclear power stations.

Such models of the environment, the detectors and the human body had to be found that serve us with a physically correct approximation but are not so complicated that the computer times became unreasonably long.

With POKER-CAMP, the code described in this report, we hope that these requirements are well satisfied.

There are certain advantages of using such calculations together with or sometimes instead of field measurements, viz.

- measurements of spectra and phantom organ doses are more time consuming and expensive than the execution of computations,

- cases that have never really happened but may occur one day can easily be analysed by the code,

- by comparing calculated and measured results, sensitivities of detectors, among other things, can be checked.

Most computer programs that are used for estimating the dose increments due to emissions from nuclear power stations follow the path of radioactive particles from emission to their dispersion in the air and/or deposition on the ground. Human doses are calculated from cloud sources and ground deposition data by using conversion factors. Such factors can easily be determined for many geometries by POKER-CAMP. Not only can they be determined more easily, our view is that they can be determined more accurately than by most of earlier methods.

2. THE MODEL

2.1 THE MODELLING OF THE ENVIRONMENT

The environment is divided into three regions (*Fig. 1*). Two semi-infinite bulks represent the air and the soil and a layer of any thickness (t in *Fig. 1*) but infinite in the two horizontal directions can also be specified between them.

The zero point of the coordinate z is at the interface between the air and the solid region(s).

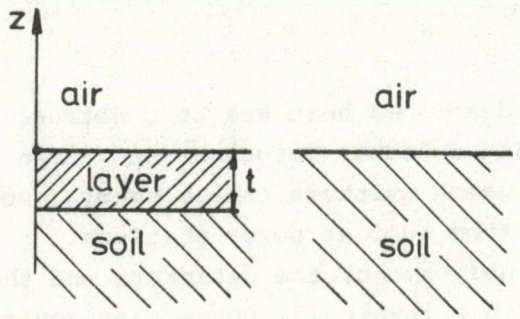

Fig.1. Geometry of the environment

The intermediate layer can be used for modelling grass, snow, etc. or simply to take into account a change in the composition of the soil. The intermediate layer can be omitted by specifying zero thickness.

The elemental composition and the density of the air are built into the code (as specified by the NBS Handbook 85 [1]); the same parameters for the other two regions must be given by the user.

2.2 RADIOACTIVE SOURCES

Three geometrical source distributions can be specified in each region (*Fig. 2*)

- uniform source
- plane source
- exponential source.

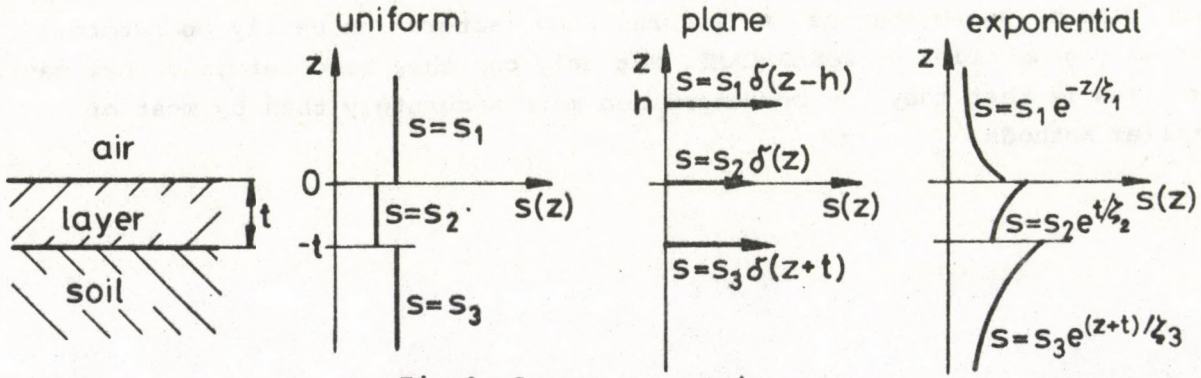

Fig.2. Source geometries

Generally, uniform distribution is a good model for natural radioactive sources in the soil.

Plane sources, which are on the real upper surfaces of the solid regions and can be set to any hight (h in *Fig. 2*) in the air, can model, for example fall-out sources.

Isotopes of fall-out washed in by rains can have specific activities decreasing exponentially by depth in the soil. The distribution of radon emanated from the soil to the air can be approximated by exponentially decreasing by height.

One can specify 10 different sources in a single task, with no change in the geometry of the environment and the composition of the soil (and layer) region(s).

Therefore if the kind of source (e.g. the isotope) is kept the same but several different source distributions are specified, more sophisticated resultant distributions can be simulated. For example, by specifying several plane sources at different heights in air, their sum approximates a cloud-profile (*Fig. 3a*). An activity concentration constant to a given depth and exponentially decreasing down from this plane can be modelled by an artifical separation of the upper layer of the soil (*Fig. 3b*).

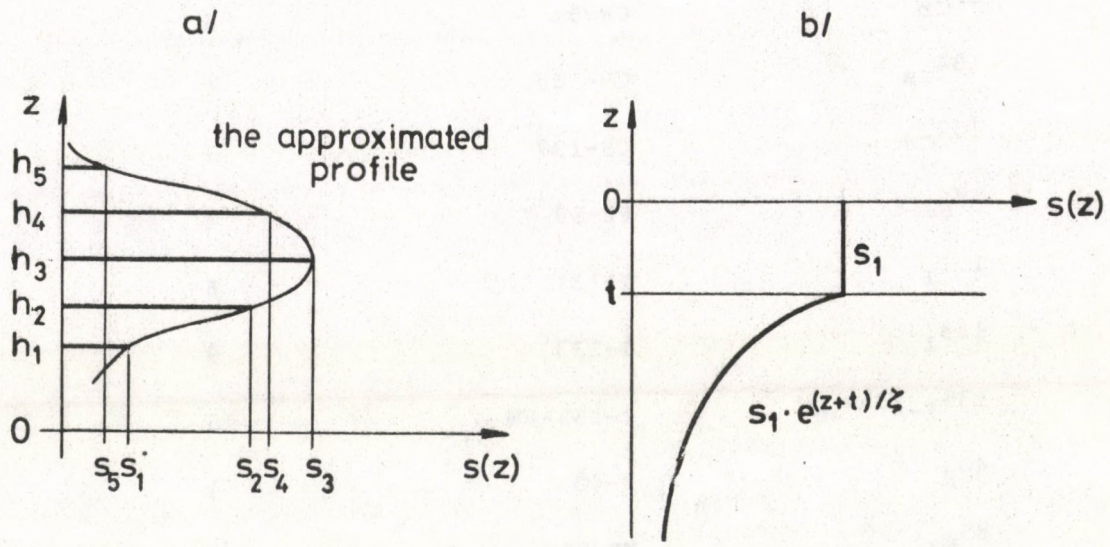

Fig.3. Examples of generation of complex source distributions by the combination of elementary ones

* * *

The energies of the different radioisotopes (or decay chains) can either be specified by the input or one can use the built-in library of the code. The line energies and intensities are catalogued for 40 sources (Table I).

Table I The radioactive sources catalogued in the code

Source	Identification word	No. of lines
^{110m}Ag	AG-110M	8
^{41}Ar	AR-41	1
^{140}Ba-^{140}La	BA-LA140	14
^{7}Be	BE-7	1
^{141}Ce	CE-141	1
^{144}Ce-^{144}Pr	CE-PR144	6
^{57}Co	CO-57	4
^{58}Co	CO-58	2
^{60}Co	CO-60	2
^{51}Cr	CR-51	1
^{134}Cs	CS-134	6
^{137}Cs	CS-137	1
^{59}Fe	FE-59	4
^{131}I	I-131	6
^{133}I	I-133	6
^{135}I-^{135m}Xe	I-135XEM	15
^{40}K	K-40	1
^{85}Kr	KR-85	1
^{85m}Kr	KR-85M	2
^{87}Kr	KR-87	8
^{88}Kr-^{88}Rb	KR-RB-88	20
^{54}Mn	MN-54	1
^{22}Na	NA-22	1

^{95}Nb	NB-95	1
^{147}Nd	ND-147	6
^{103}Ru	RU-103	4
^{106}Ru-^{106}Rh	RU-RH106	4
^{124}Sb	SB-124	10
^{125}Sb	SB-125	7
^{123m}Te	TE-123M	1
^{131m}Xe	XE-131M	1
^{133}Xe	XE-133	2
^{133m}Xe	XE-133M	1
^{135}Xe	XE-135	3
^{135m}Xe	XE-135M	1
^{138}Xe	XE-138	14
^{65}Zn	ZN-65	1
^{95}Zr	ZR-95	2
U-Ra decay series	RA-CHAIN	24
Th decay series	TH-CHAIN	20

This gamma energy catalogue of the program was constructed on basis of the work of Reus et al. [2]. In their original publication there are many more energy lines of several isotopes and decay chains than in our catalogue but we have managed to reduce the data thereby leading to a saving in computer time. We combined lines where the intensity of one was much less than that of the nearest neighbour or if the difference in the energies of two (or more) lines was very small. Even though we realize that there is a certain amount of subjectivity involved in this simplification, as a rule of thumb we can state that lines deviating in energy by more than 10 per cent were combined only if the intensity of one was less than 3 per cent of that of the next one.

If n lines with energies E_i and intensities I_i were combined, then the resultant energy E and intensity I were calculated as

$$E = \frac{\sum_{i=1}^{n} E_i I_i}{I}, \qquad I = \sum_{i=1}^{n} I_i .$$

The content of this catalogue can be printed out (see Section 4.1); the user can modify it by changing the values in the BLOCK DATA segment placed after the SUBROUTINE EDITGL (for details see Section 4.3).

2.3 DETECTORS

There are four types of detectors (or targets) handled by POKER-CAMP:
- points, or point-like detectors
- cylindrical detectors
- spherical phantoms
- anthropomorphic phantoms.

2.3.1 Point-like detectors

A detection-point can be placed at any height in the air or depth in the soil (or layer) (z_D), or it can be located on the trunk of a male phantom (*Fig. 4*).

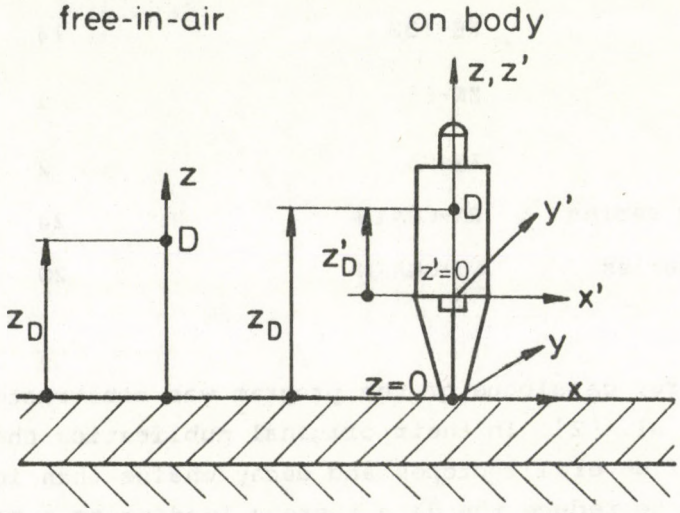

Fig.4. Setting of the point-like detectors

On the phantom the detector is located on the median line of the trunk at the front (x' = 0, where x' is one of the horizontal coordinates in the system fitted to the phantom, (see Section 3.1)). The vertical position can be anywhere on the trunk ($0 \leq z'_D \leq 70$ cm). The phantom itself will be described later (Subsection 2.3.4), here in the further comments on the detectors there is no difference between the free-in-air (or in-soil) and on-body points.

The code always calculates the flux density at the point investigated together with the air kerma rate and the average energy of the photons ($\bar{E}$):

$$\bar{E} = \int E\Phi(E)\,dE \Big/ \int \Phi(E)\,dE$$

The user can also ask for the spectra of the photons: the flux and the kerma rate spectra can be calculated for $N_E \leq 30$ energy groups (equal intervals from the low energy limit to the maximum source energy) and/or $N_\vartheta \leq 30$ angular segments (where the angles of the group limits measured from the positive z or y axes are equidistributed at $0\text{-}180^\circ$).

In the case of physical detectors, their responses depend generally on the energy and/or the angle of incidence of the photons. The responses of such detectors can also be calculated in several ways by POKER-CAMP. In the most general case the response (R) is a functional of the flux (ϕ), i.e.:

$$R = \int dE \int d\vartheta \gamma(E,\vartheta)\phi(E,\vartheta). \qquad (2.1)$$

Several points of the $\gamma(E,\vartheta)$ sensitivity function can be arranged in a matrix,

$$\overline{\overline{M}}\{m_{ij} = \gamma(E_i,\vartheta_j)\}, \qquad (2.2)$$

where E_i and ϑ_j are user-selected base points. The program accepts a maximum of 900 elements ($i \leq 30$, $j \leq 30$) and the user can specify the unit of quantity R which is formed by the function.

In many cases the detector sensitivity is more easily related to the dose rate; in such cases another sensitivity function γ^* is introduced:

$$R = \int dE \int d\vartheta \gamma^*(E,\vartheta)\dot{K}(E,\vartheta) \quad , \qquad (2.3)$$

and the matrix elements are:

$$m^*_{ij} = \gamma^*(E_i,\vartheta_j). \qquad (2.4)$$

The angle of incidence (ϑ) can be measured either from axis z or from axis y (this means any horizontal direction in the free-in-air case, when there is a cylindrical symmetry of the problem, and means the direction perpendicular to the middle of the chest of the phantom if it is involved). In each case an azimuth independence is assumed.

There may be cases when the energy and angular dependences are separatable:

$$R = \int dE\alpha(E) \int d\vartheta\beta(\vartheta)\phi(E,\vartheta), \qquad (2.5)$$

or

$$R = \int dE\alpha^*(E) \int d\vartheta\beta^*(\vartheta)\dot{K}(E,\vartheta). \qquad (2.6)$$

and thus instead of the matrices simpler vectors can be used:

$$\bar{\alpha}\{\alpha_i = \alpha(E_i)\}, \quad \text{or} \quad \bar{\alpha}^*\{\alpha_i^* = \alpha^*(E_i)\}$$

and

$$\bar{\beta}\{\beta_j = \beta(\vartheta_j)\}, \quad \text{or} \quad \bar{\beta}^*\{\beta_j^* = \beta^*(\vartheta_j)\},$$

with the restriction $i \leq 30$, $j \leq 30$.
In the simplest case the response of the detector is independent of the photons' energy or of the angle of incidence, i.e.

$$\alpha(E) \equiv \alpha^*(E) \equiv 1,$$

or

$$\beta(\vartheta) \equiv \beta^*(\vartheta) \equiv 1,$$

so the specification of one vector is enough.

The sensitivity values for energies and/or angles lying between two user-selected base points are calculated by linear interpolation. For energies or angles below the lowest base point value or above the highest base point, the sensitivities regarding the lowest or highest base points are used, respectively (*Fig. 5*).

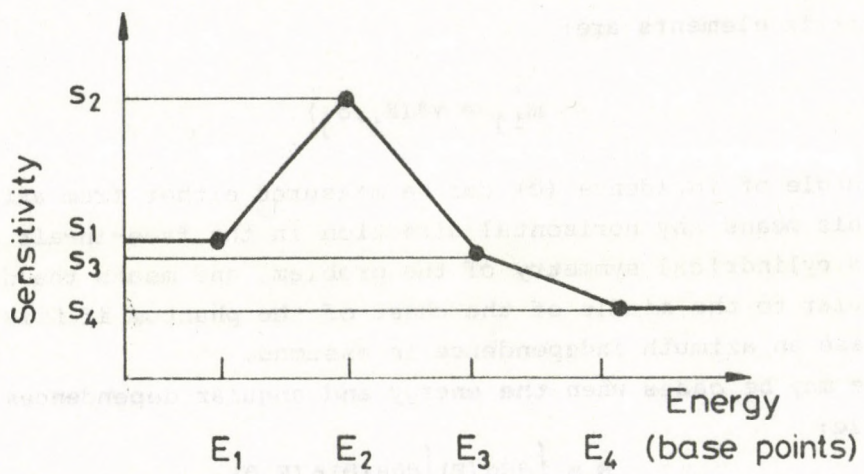

Fig.5. Simple scheme of an interpolated sensitivity curve

Since the calculation of a response needs only the multiplication by the actual sensitivity and does not influence the whole simulation process, as many as 10 special detector responses can be computed in a single task.

2.3.2 Cylindrical detectors

The symmetry axis of the cylindrical detectors must coincide with the coordinate z (*Fig. 6*) of the environment. The height (h) and the radius (r), the elemental composition and the density of the detector material are input data together with the vertical coordinate of the centre (z_D).

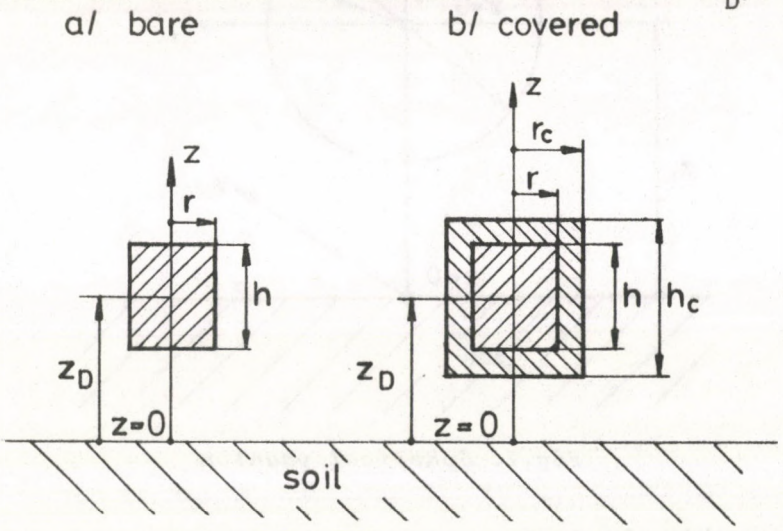

Fig.6. Cylindrical detectors

Besides bare detectors, covered ones can also be investigated, in which case the height (h_c), the radius (r_c) and the material of the cover must also be specified. The geometrical centre of the cover has to coincide with that of the actual detector.

The whole cylindrical detector must be in the air, i.e.

$$z_D \geq h/2, \quad \text{or} \quad z_D \geq h_c/2.$$

The average flux and the kerma rate in the (actual) detector are calculated.

By this mode, for example total efficiencies of scintillation crystals can be calculated.

2.3.3 Spherical phantoms

A sphere of any dimensions and material can also be put in air ($z_D \geq r$, *Fig. 7*) and the program calculates the flux and the kerma rate for any point (P: z_1' , x_1') inside the sphere ($z_1'^2 + x_1'^2 \leq r^2$) or for the total sphere. In the latter case the flux density is also averaged over the whole sphere.

This detection mode can be used, for example, for calculating doses in the ICRU [3] 30 cm diameter sphere and hence, by calculations repeated for a series of points inside the sphere, one can determine the dose index. (It is for this reason that we call this target "spherical phantom" rather than "spherical detector".)

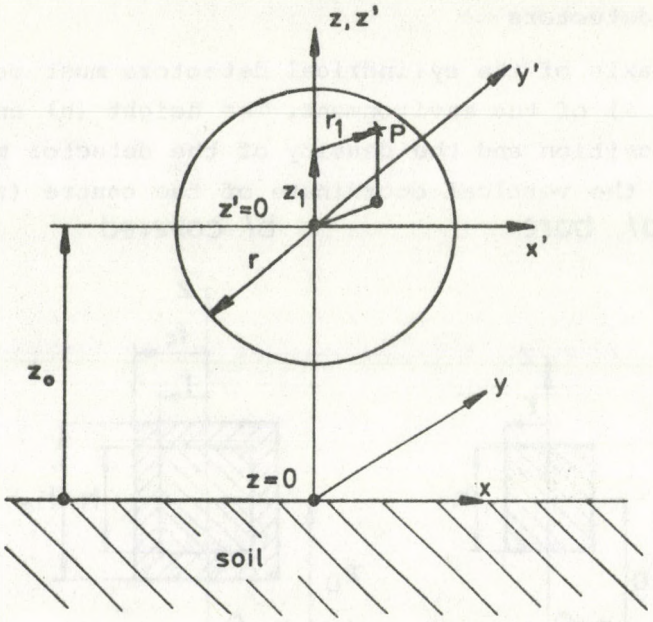

Fig.7. Spherical phantom

2.3.4 Anthropomorphic phantoms

In this mode a male or a female phantom can stand on the ground (on the top of the soil, or on the intermediate layer, if it is included).

The ORNL mathematical phantom was first described and later modified by Snyder et al. [4,5]. This phantom was a hermaphrodite, so it had both sets of genitals but no breasts. Because, in the new limitation system, the breasts have increased importance, Cristy has provided the original phantom with breasts [6]. In POKER-CAMP there are two types of phantoms: the original, now called "male" as described in [5] and the "female" which has breasts but has no "genitalia region", i.e. the region covering the testicles (*Fig. 8*). Otherwise the two phatoms are identical.

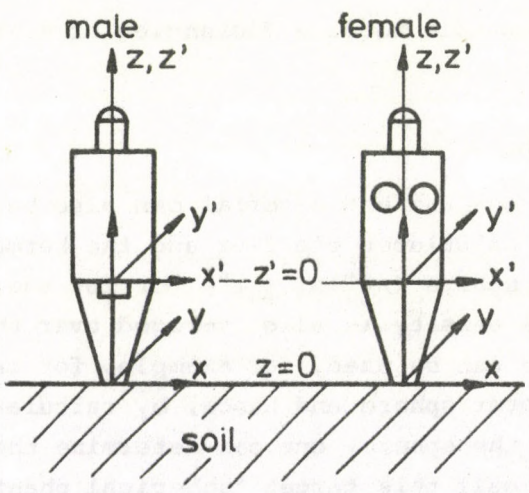

Fig.8. Anthropomorphic phantoms

ORNL phantoms have relatively simple geometrical shapes. The external surfaces and the boundaries of the more than 20 organs are defined by secondary order equations. Each organ is considered to be homogeneous although different elemental compositions and densities are used for the skeleton, the lungs and the remainder of the phantom.

In Table II target organs that can be selected are listed.

Besides the calculation of the doses absorbed in several separate organs there is a possibility to estimate directly the effective dose equivalent. This is an advantage of the adjoint Monte Carlo simulation used in POKER-CAMP that the weighted average of the organ doses is computable without the calculation of the single organ doses themselves (see also Subsection 3.2.1).

ICRP Report 26 [7] recommends the use of the quantity "effective dose equivalent" (H_E) as the base in the dose limitation for stochastic effects. The effective dose equivalent is a weighted sum of several tissues (Table III).

Table II Target organs

Ident. no.	Organ	Male phantom	Female phantom
1	Whole body	+	+
2	Testicle	+	-
3	Ovary	-	+
4	Red bone marrow	+	+
5	Yellow bone marrow	+	+
6	Lung	+	+
7	Thyroid	+	+
8	Breast	-	+

Table III Weights for determining H_E in accordance with ICRP 26

Tissue	Weight
Gonads	0.25
Breast	0.15
Red bone marrow	0.12
Lung	0.12
Thyroid	0.03
Bone surfaces	0.03
Remainder	0.30

In POKER-CAMP two approximations had to be made.

1/ There are no "bone surfaces" in the ORNL phantom, therefore its very slight (3 per cent) contribution is replaced by the dose of the red bone marrow.

2/ For the "remainder" the ICRP recommends that a weight of 0.06 is applicable to each of the five organs or tissues of the remainder receiving the highest dose. Instead of this, total body dose is calculated by the code. It is hoped that in environmental exposures, where the dose is quite homogeneously distributed in the body, this approximation does not lead to significant errors.

For the organs that are present in both sexes the calculation is carried out in half of the cases for the male and half of the cases for the female phantom. The weighting factors used in POKER-CAMP to estimate the effective dose equivalent are given in Table IV.

Table IV Weights used for computing H_E by the code

Tissue	Weights for male phantom	Weights for female phantom
Testicle	0.125	-
Ovary	-	0.125
Breast	-	0.15
Red bone marrow	0.075	0.075
Lung	0.06	0.06
Thyroid	0.015	0.015
Whole body	0.15	0.15

3. THE ADJOINT MONTE CARLO PROCEDURES

3.1 COORDINATE SYSTEMS

POKER-CAMP works always in Cartesian coordinates. The z axis points upwards, goes through the point-like detector (if it is not placed on the phantom) or the centre of the cylindrical or spherical detectors or the centre of the anthropomorphic phantom's trunk. The centre of the coordinate system is located at the top of the solid regions, i.e. the soil bulk or the intermediate layer - if it exists (see *Figs. 4, 6, 7 and 8*).

Unless a phantom is standing in the system the orientation of x and y coordinates has no physical meaning since the geomerty is cylindrically symmetrical. If a phantom is investigated, the x coordinate is directed from the phantom's right to the left (left organs have positive x coordinates), the y axis points from the front of phantom to the back (see *Fig. 8*).

If an anthropomorphic phantom is involved (either as target or as a holder of a point-like detector), then another system, that of the phantom-coordinates (x', y' and z' on *Figs. 3 and 7*), is introduced. The axes z and z'coincide but z' = 0 is set to z = 80, i.e. on the plane separating the legs from the trunk, therefore the z' = z - 80 transformation holds. The axes x' and y' are parallel to x and y, respectively and x' = x, y' = y.

3.2 ADJOINT TRANSPORT EQUATIONS AND THEIR SOLUTION BY MONTE CARLO

A short overview is presented in this section on the adjoint transport equations and their solution by Monte Carlo techniques. No details of the basic theory are presented here, those who wish for a deeper insight should refer to, for example, the excellent review by Irving [8].

Let us start with the collision density equations:

$$\chi(\bar{r},\bar{E}) = S(\bar{r},\bar{E}) + \int d\bar{E}'C(\bar{E}',E|\bar{r})\psi(\bar{r},\bar{E}') \qquad (3.1)$$

and

$$\psi(\bar{r},\bar{E}) = \int d\bar{r}'T(\bar{r}',\bar{r}|\bar{E})\chi(\bar{r}',\bar{E}) \qquad (3.2)$$

where χ and ψ are respectively the collision densities of particles leaving, or entering a collision at $\bar{r}$ with energy E and direction of flight $\bar{\omega}$. (To simplify the notation, $\bar{E}$ is used instead of $(E,\bar{\omega})$.) $S(\bar{r},\bar{E})$ denotes the source density, T is the transport kernel:

$$T(\bar{r}',r|\bar{E}) = \mu(\bar{r},E)\exp\left[-\int_{\bar{r}'\to\bar{r}} \mu(\bar{r}'',E)ds\right] \frac{\delta\left(\bar{\omega}\frac{\bar{r}-\bar{r}'}{|\bar{r}-\bar{r}'|} - 1\right)}{|\bar{r}-\bar{r}'|^2} ,$$

where μ is the linear attenuation coefficient.

Here $\int_{\bar{r}'\to\bar{r}} \mu(\bar{r}'')ds$ is a symbol for integration along the line from $\bar{r}'$ to $\bar{r}$.

If we introduce a new variable R′ being O at $\bar{r}'$ and R at $\bar{r}$; that is any point along the $\bar{r}'\to\bar{r}$ line is discribable as

$$\bar{r}'' = \bar{r}' + R'\bar{\omega} ,$$

then the general transport operation can be replaced by a one dimensional integration:

$$T\varphi(\bar{r}',\bar{E}) = \int dR\mu(\bar{r}'+R\bar{\omega},E)\exp\left[-\int_0^R \mu(\bar{r}'+R'\bar{\omega},E)\,dR'\right]\varphi(\bar{r}',E) . \qquad (3.3)$$

C is the collision kernel:

$$C(\bar{E}',\bar{E}|\bar{r}) = \frac{\mu_s(\bar{r},\bar{E}'\to\bar{E})}{\mu(\bar{r},E')} ,$$

where μ_s is the differential linear scattering coefficient. In our case the scattering angle is fully determined by the energy change, therefore μ_s can be factorized as

$$\mu_S(\bar{r},\bar{E}'\to\bar{E}) = f_E(\bar{r},E'\to E)\,\delta[\bar{\omega}'\bar{\omega}-g(E',E)] . \qquad (3.4)$$

The azimuth of the scattering is assumed to be equidistributed on $(O;\ 2\pi)$. The actual form of $g(E',E)$ depends on the type of scattering (see Section 3.5).

The physical quantity to be determined (λ) is a functional of one of the collision densities, e.g.:

$$\lambda = \iint d\bar{r}d\bar{E}P_\psi(\bar{r},\bar{E})\psi(\bar{r},\bar{E}) .$$

The actual form of the P_ψ pay-off function is determined by the physical meaning of the actual λ.

If the flux-at-a-point $\varphi(\bar{r}_o)$ is to be calculated, then by taking into account the relation between the flux and the collision density:

$$\psi(\bar{r},\bar{E}) = \mu(\bar{r},E)\varphi(\bar{r},\bar{E}) ,$$

$\varphi(\bar{r}_o)$ can be calculated as

$$\varphi(\bar{r}_o) = \int d\bar{E}\varphi(\bar{r}_o,\bar{E}) = \int d\bar{E}\mu^{-1}(\bar{r}_o,E)\psi(\bar{r}_o,\bar{E}) ,$$

i.e.

$$P_\psi(\bar{r},\bar{E}) = \mu^{-1}(\bar{r},E)\,\delta(\bar{r}-\bar{r}_o) . \qquad (3.5)$$

A direct Monte Carlo simulation can be based on Eqs.(3.1)-(3.5) but for cases where the source region is much more extended in space than the target, the so-called adjoint Monte Carlo method is generally more efficient. To derive the equations which serve as a basis for the POKER-CAMP calculations let us introduce two new functions. $\chi^*(\bar{r},\bar{E})$ and $\psi^*(\bar{r},\bar{E})$, representing the value of a particle just leaving or entering a collision, respectively.

The value is a sum of the immediate pay-off and the pay-off that is expected to result from all future collisions. Obviously the pre- and post-collisions are interdependent according to the equations:

$$\psi^*(\bar{r},\bar{E}) = P_\psi(\bar{r},\bar{E}) + \int d\bar{E}' C(\bar{E},\bar{E}'|\bar{r})\chi^*(\bar{r},\bar{E}')$$

and

$$\chi^*(\bar{r},\bar{E}) = \int d\bar{r}' T(\bar{r},\bar{r}'|\bar{E})\psi^*(\bar{r}',\bar{E}).$$

The physical quantity can now be determined as

$$\lambda = \iint d\bar{r}d\bar{E}\psi^*(\bar{r},\bar{E})S_c(\bar{r},\bar{E}),$$

where

$$S_c(\bar{r},\bar{E}) = \int d\bar{r}' T(\bar{r}',\bar{r}|\bar{E})S(\bar{r}',\bar{E}), \qquad (3.6)$$

is the first collision source.

An equation system more suited to Monte Carlo simulation can be derived by introducing the modified functions:

$$\hat{\psi}(\bar{r},\bar{E}) = \mu(\bar{r},E)\psi^*(\bar{r},-\bar{E}),$$
$$\hat{\chi}(\bar{r},\bar{E}) = \mu(\bar{r},E)\chi^*(\bar{r},-\bar{E}),$$
$$\hat{P}_\psi(\bar{r},\bar{E}) = \mu(\bar{r},E)P_\psi(\bar{r},-\bar{E})$$

and

$$\hat{C}(\bar{E},\bar{E}'|\bar{r}) = C(\bar{E},\bar{E}'|\bar{r})\,\frac{\mu(\bar{r},E)}{\mu(\bar{r},E')} = \frac{\mu_s(\bar{r},\bar{E}\to\bar{E}')}{\mu(\bar{r},\bar{E}')}.$$

The modified value equations are now:

$$\hat{\psi}(\bar{r},\bar{E}) = \hat{P}_\psi(\bar{r},\bar{E}) + \int d\bar{E}'\hat{C}(\bar{E},\bar{E}'|\bar{r})\hat{\chi}(\bar{r},\bar{E}') \qquad (3.7)$$

$$\hat{\chi}(\bar{r},\bar{E}) = \int d\bar{r}' T(\bar{r}',\bar{r}|\bar{E})\hat{\psi}(\bar{r}',\bar{E}) \qquad (3.8)$$

and the quantity of interest can be determined by

$$\lambda = \iint d\bar{r}d\bar{E}\hat{\psi}(\bar{r},\bar{E})\frac{S_c(\bar{r},-\bar{E})}{\mu(\bar{r},E)}. \qquad (3.9)$$

Both the value and the modified value equations are generally called adjoint equations.

* * *

The Monte Carlo solution of Eqs. (3.7)...(3.9) can easily be illustrated by the introduction of so-called pseudo-photons whose transport is governed by just the above mentioned equations. The theoretical frame of this simulation process is the following:

Step 1: Selection of the initial coordinates of $\bar{r}'$ and $\bar{E}'$ from the normalized pay-off function:

$$\frac{\hat{P}_\psi(\bar{r}',\bar{E}')}{\int\int d\bar{r}d\bar{E}\hat{P}_\psi(\bar{r},\bar{E})}$$

and setting an initial statistical weight to the pseudo-photon as

$$\int\int d\bar{r}d\bar{E}\hat{P}_\psi(\bar{r},\bar{E}).$$

Step 2: Simulation of the free flight of the pseudo photon: Choose the path length R from (see Eq. (3.3)):

$$f(R) = \mu(R)\exp\left[-\int_0^R \mu(R')dR'\right], \quad R' \geq 0 . \tag{3.10}$$

(In our case, where $\mu(\bar{r})$ is nonvanishing $f(R)$ is always a probability density function; i.e. $\int_0^\infty f(R)dR = 1$, therefore there is no need for any normalization.) The new coordinates are $\bar{r} = \bar{r}' + R\bar{\omega}'$.

Step 3: Selection of the energy and direction of flight after the scattering of the pseudo-photon. Choose E from the normalized scattering kernel:

$$\frac{\hat{C}_E(E,E'|\bar{r})}{\int dE\hat{C}_E(E,E'|\bar{r})}$$

and multiply the statistical weight of the pseudo-photon by

$$\int dE\hat{C}_E(E,E'|\bar{r}). \tag{3.11}$$

Here the energy E, from which a real photon should have been scattered to E', is selected. Therefore the energy of a pseudo-photon increases at every pseudo-scattering event.

The subscript E in $\hat{C}_E$ indicates that here only the energy change is considered; the change in the angle is determined through the function $g(E',E)$ introduced in Eq.(3.4), therefore

$$\hat{C}(\bar{E},\bar{E}'|\bar{r}) = \hat{C}_E(E,E'|\bar{r})\delta[\bar{\omega}\bar{\omega}'-g(E,E')].$$

Choose $\bar{\omega}$ so that $\bar{\omega}\bar{\omega}' = g(E,E')$ (see Eq.(3.4) and the comment following it).

Step 4: Set

$$\bar{r}' = \bar{r}$$

$$\bar{E}' = \bar{E}$$

and return to Step 2.

A history is terminated if the pseudo-photon's energy becomes larger than the maximum source energy.

This procedure corresponds to the calculation of estimates for the von Neumann series for the modified value functions.
Step 1 produces

$$\hat{\psi}_o(\bar{r}',\bar{E}') = \hat{P}_\psi(\bar{r}',\bar{E}'), \tag{3.12}$$

Steps 2 to 4 correspond to calculating:

$$\hat{\chi}_1(\bar{r},\bar{E}') = \int d\bar{r}' T(\bar{r}',\bar{r}|\bar{E}')\hat{\psi}_o(\bar{r}',\bar{E}')$$

and

$$\hat{\psi}_1(\bar{r},\bar{E}) = \int d\bar{E}'\hat{C}(\bar{E},\bar{E}'|\bar{r})\hat{\chi}_1(\bar{r},\bar{E}').$$

Then by returning to Steps 2 and 3

$$\hat{\chi}_i(\bar{r},\bar{E}') = \int d\bar{r}' T(\bar{r}',\bar{r}|\bar{E}')\hat{\psi}_{i-1}(\bar{r}',\bar{E}')$$

and

$$\hat{\psi}_i(\bar{r},\bar{E}) = \int d\bar{E}'\hat{C}(\bar{E},\bar{E}'|\bar{r})\hat{\chi}_i(\bar{r},\bar{E}')$$

are calculated.
After terminating all histories the modified value functions are obtained by summing the von Neumann series:

$$\hat{\chi}(\bar{r},\bar{E}) = \sum_{i=1}^{\infty} \hat{\chi}_i(\bar{r},\bar{E})$$

and

$$\hat{\psi}(\bar{r},\bar{E}) = \sum_{i=o}^{\infty} \hat{\psi}_i(\bar{r},\bar{E}). \tag{3.13}$$

By this simulation the collision densities are generated. For our final purpose the physical quantity of interest must be calculated, so scoring has to be made at every pseudo-scattering event on the basis of (3.9).

Details of the simulation process and the scoring are described in the following sections.

3.2.1 Selection of the starting coordinates

By Eq. (3.5) the pay-off function was derived for the flux-at-a-point estimation. This pay-off is used when the point-like detectors are investigated. So in those cases the initial spatial coordinate is simply set to the detector coordinates:

$$z_o = z_D$$

$$x_o = y_o = 0.$$

If the target is homogeneous but is extended in space, then the quantity to be estimated is the flux averaged over the target volume (V_T):

$$\hat{P}_\psi(\bar{r},\bar{E}) = \frac{1}{V_T} \int_{V_T} d\bar{r}_o \delta(\bar{r}-\bar{r}_o), \qquad (3.14)$$

i.e. the initial point $\bar{r}_o$ must be selected with equal probability from any point of the target volume. There are several methods described in the literature for such random selection (see e.g. [9]). In the POKER-CAMP code points from simple geometrical volumes (e.g. cylinders, spheres) are selected by direct sampling (inverting the cumulative distribution functions); for more sophisticated volumes (phantom organs) rejection techniques are used.

The skeleton of the phantoms is divided into 13 segments (bones and bone parts) having different marrow contents, and the distribution of the marrow tissues is uniform within each segment. Thus, if the target is the marrow, first a bone segment is selected (with a probability proportional to its marrow content), and then the starting point is chosen from its volume.

For the phantom dose calculations the really important quantity is not the flux integral but the dose absorbed (the flux-to-dose conversion is described in Section 3.4). The dose absorbed in a target can - by definition - be calculated by averaging over the total mass (and not simply the volume) of the target. Therefore for heterogeneous targets we average the flux also over the mass, i.e. instead of (3.14) a density weighted average is made:

$$\hat{P}_\psi(\bar{r},\bar{E}) = \frac{1}{m_T} \int_{V_T} d\bar{r}_o \rho(\bar{r}_o) \delta(\bar{r}-\bar{r}_o),$$

where m_T is the mass of the target.

The whole body of the phantom is inhomogeneous, the densities of the three types of tissues are different from each other. Here a uniform random selection is carried out for the whole phantom volume but the initial statistical weight is multiplied by the density of the region where the selected point lies.

If the effective dose equivalent is calculated, then the organs and the sex of the phantom are selected randomly but the selection probabilities are equal to the weights given in Table IV.

Initial energies are uniformly selected from the interval

$$E_{max} - E_{min},$$

where E_{max} is the maximum source energy and

E_{min} is the low energy limit, i.e. the energy below which the contribution of the photons is assumed to be negligible (suggested value: ~10-20 keV).

The initial direction of flight is selected randomly on the 4π solid angle.

Since

$$\int_0^{4\pi} d\bar{\omega} \int_{E_{min}}^{E_{max}} dE \hat{P}_\psi(\bar{r},\bar{E}) = 4\pi (E_{max}-E_{min}) \hat{P}_\psi(\bar{r},\bar{E}),$$

the initial weight of each particle must be multiplied by

$$4\pi (E_{max} - E_{min}).$$

3.2.2 Path length selection

In simple geometries (if the phantom is not involved) the free path length (R) can be selected from distribution (3.10) simply by inverting the cumulative distribution function, i.e. if there are n regions of different materials and attenuation coefficients that can be crossed by the pseudo-particle (*Fig. 9*),

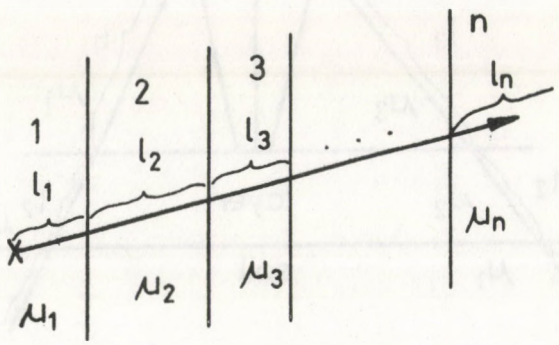

Fig.9. Sketch of the path length selection in simple geometries

then the region i in which the next collision takes place is determined by

$$\sum_{j=1}^{i-1} \mu_j \ell_j < -\ln r < \sum_{j=1}^{i} \mu_j \ell_j ,$$

where r is a random number equidistributed on (0, 1) and ℓ_j is the pseudo-photon's trajectory in region j (j = 1, 2,..,i-1). The path length is calculated as

$$R = \sum_{j=1}^{i-1} \ell_j + \frac{-\ln r - \sum_{j=1}^{i-1} \mu_j \ell_j}{\mu_i} . \qquad (3.15)$$

For a phantom standing on the ground, the paths that do not cross it are selected by the above mentioned method, however for paths crossing the phantom the determination of the boundaries where the material changes (i.e. the determination of crossing points of the path with secondary order surfaces separating the phantom regions) becomes extremely complicated and time consuming. Instead, the following three step procedure is applied:

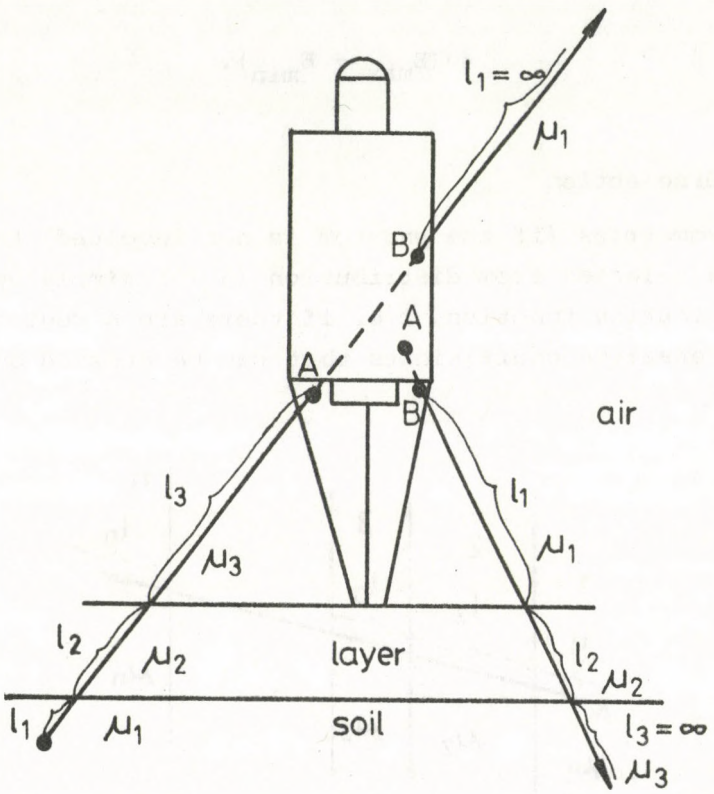

Fig.10. Sketch of the path length selection for paths crossing the anthropomorphic phantoms

a/ Select a random number r and take its negative logarithm:

$$\gamma = - \ln r.$$

Assume that the direction of the pseudo-photon crosses m regions (j=1,2,..,m) before reaching the phantom. Now, if

$$\gamma < \sum_{j=1}^{m} \mu_j \ell_j ,$$

then the simple procedure described above is applied and the free path length is calculated by (3.15). Otherwise:

b/ move the pseudo-photon to the point where it starts to fly in the phantom (points A in *Fig. 10*) and select a potential next collision site by using the maximum attenuation coefficient μ_{max}; in our case the coefficient of the bone. Then the ratio of $p = \mu_{pot}/\mu_{max}$ is calculated (μ_{pot} denotes the attenuation coefficient at the selected potential site) and with a probability of p the site is regarded as a real collision point, while with the probability 1-p a new path starting from the potential site is selected, with the same direction and μ_{max} again. If during this recursive process the pseudo-photon leaves the phantom before a real collision point is found, then:

c/ put the pseudo-photon to the point where the path goes out of the phantom (points B in *Fig. 10*) and select an additional free path by (3.15).

If the pseudo-photon starts from just inside the body, the path length selection starts tivially by step b.

3.2.3 New energy selection

In POKER-CAMP the scattering event is always assumed to be fully descirbed by the Klein-Nishina formula of the Compton-scattering process (see 3.4.2). By this formula the execution of Step 3 of the simulation (Section 3.2) is rather problematic since the integral $\int dE \, \hat{C}_E(E,E'|\bar{r})$ may be divergent. Therefore a biased energy transfer kernel

$$\hat{C}^*_E(E,E'|\bar{r}) = \frac{E'}{E} \hat{C}_E(E,E'|\bar{r})$$

is used and the statistical weight is multiplied by E/E' after each collision. Thus there is no problem with the selection of the new energy because the integral of $\hat{C}^*_E$ in terms of E is finite and the final result is unbiased - due to the weight correction. Details of the energy selection technique are given elsewhere [10].

3.2.4 Scoring

The sum of the collision density series terms in (3.13) can be separated into two parts: the first ($\hat{\psi}_o$) is due to the uncollided pseudo-photons, the second term comprises the contributions of all the later collisions:

$$\hat{\psi} = \hat{\psi}_o + \hat{\psi}', \quad \hat{\psi}' = \sum_{i=1}^{\infty} \hat{\psi}_i .$$

Hence, the physical quantity of interest (3.9) is also a sum of two contributions:

$$\lambda = \lambda_o + \lambda' ,$$

$$\lambda_o = \varphi_o(\bar{r}_o) = \iint d\bar{r}d\bar{E}\hat{\psi}_o(\bar{r},\bar{E}) \frac{S_c(\bar{r},-\bar{E})}{\mu(\bar{r},E)} \tag{3.16}$$

and

$$\lambda' = \sum_{i=1}^{\infty} \lambda_i = \sum_{i=1}^{\infty} \iint d\bar{r}d\bar{E}\hat{\psi}_i(\bar{r},\bar{E}) \frac{S_c(\bar{r},-\bar{E})}{\mu(\bar{r},E)} . \tag{3.17}$$

It is easy to prove that the contribution of the uncollided pseudo-photons equals to that of the uncollided photons, the contribution of the physical photons that reach the detector without collision. Therefore these results can directly be compared with, for example, full-energy-peak efficiencies of scintillation detectors.

Let us further deduce the source term (3.16). If we first assume an isotropic and monoenergetic source with a geometrical distribution of $S_g(\bar{r})$, then

$$S(\bar{r},\bar{E}) = \frac{1}{4\pi} \delta(E-E_o) S_g(\bar{r}). \tag{3.18}$$

By this expression and relation (3.12)

$$\lambda_o = \int d\bar{\omega} \frac{1}{4\pi} \int d\bar{r}' \mu^{-1}(\bar{r}_o,E_o) T(\bar{r}',\bar{r}_o|E_o,\bar{\omega}) S_g(\bar{r}') ,$$

i.e. if an initial direction $\bar{\omega}_o$ is selected from the uniform distribution, then the score (s) is:

$$s = \ell(\bar{r}_o,E_o,\bar{\omega}_o) = \int d\bar{r}' \mu^{-1}(\bar{r}',E_o) T(\bar{r}_o,\bar{r}'|E_o,-\bar{\omega}_o) S_g(\bar{r}'). \tag{3.19}$$

The integration is extended over the whole source region, in other parts of the space $S_g(\bar{r}') \equiv 0$.

For a further analysis of integral (3.19) let us turn again to the one dimensional form, similarly to that used for the derivation of (3.3) and by

introducing the $s(R)$ function for describing the source change along axis R. Then, by the notation of *Fig. 11*, the integral ℓ is:

$$\ell = \int_{R_1}^{R_2} dR \exp\left[-\int_{o}^{R} \mu(R')\,dR'\right] s(R) =$$

$$= \underbrace{\exp\left[-\int_{o}^{R_1} \mu(R')\,dR'\right]}_{p} \cdot \underbrace{\int_{R_1}^{R_2} dR \exp\left[-\int_{R_1}^{R_2} \mu(R')\,dR'\right] s(R)}_{L}.$$

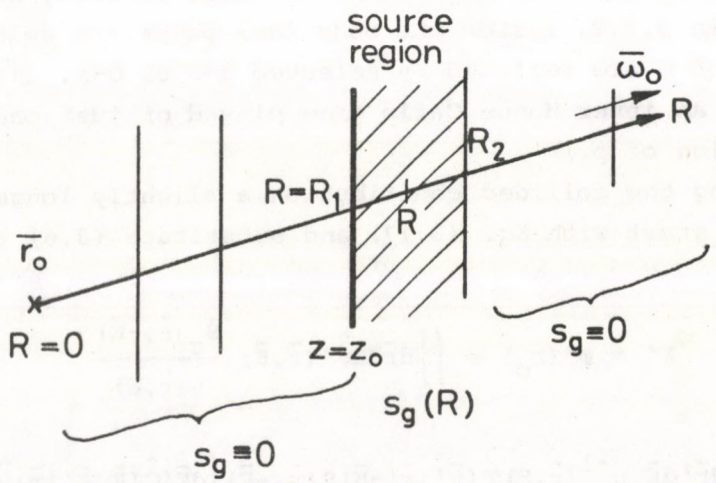

Fig.11. The score along a path

Here, the first factor (p) is the probability that the pseudo-photon reaches the source region, being trivially 1, if the path starts from the source region.

The meaning of the second factor (L) depends on the type of source distribution. For uniform distribution: $s(R) \equiv S_o$, L is just the expected path-length in the source region of a pseudo-photon assuming that it reached this region (this assumption is trivially fulfilled if the path starts from the source region).

For an exponentially decreasing source intensity:

$$S_g(z) = S_o e^{(z-z_o)/\zeta},$$

L is also a track-length type quantity but for the calculation of the expected length

S_o must be replaced by $S_o e^{(z_1-z_o)/\zeta}$

where z_1 is the point where the path enters the source region and

μ must be replaced by $\mu + \omega_z/\zeta$

where ω_z is the z component of $\bar{\omega}$.

For a surface source

$$S_g(z) = S_o \delta(z-z_o),$$

L is simply $S_o/|\omega_z|$.

Since there is some similarity in the physical meanings of the three types of integral ℓ, in the following all of them will be referred to as "track-length type factor" of the score.

The evaluation of L is always carried out analytically. The source-region-reaching probability p is also evaluated analytically if there is no anthropomorphic phantom but the determination of the probability of coming out of the body would take too much computer time. Instead, similarly to the method described in 3.2.2, inside the body real paths are selected and therefore values of p are replaced by selected 1-s or 0-s. (This method can be interpreted as an inner Monte Carlo game played of just one experiment for the determination of p.)

For estimating the collided contribution a slightly longer derivation is needed. Let us start with Eq. (3.17) and substitute (3.6) and (3.7) into it:

$$\lambda' = \varphi'(\bar{r}_o) = \iint d\bar{r} d\bar{E} \hat{\psi}'(\bar{r},\bar{E}) \frac{S_c(\bar{r},-\bar{E})}{\mu(\bar{r},E)}$$

$$= \iiint d\bar{r} d\bar{r}' d\bar{E}\ \mu^{-1}(\bar{r},E) T(\bar{r}',\bar{r}|-\bar{E}) S(\bar{r},-\bar{E}) \int d\bar{E}' \hat{C}(\bar{E},\bar{E}'|\bar{r}) \hat{\chi}(\bar{r},\bar{E}').$$

(It may be curious in this equation that the argument $\bar{r}_o$ does not appear explicitly on the right-hand side but $\hat{\psi}$ and $\hat{\chi}$ depend on $\bar{r}_o$ through $\hat{\chi}_1 = T(\bar{r}_o,\bar{r}|\bar{E})$. In other words the distribution of the pseudo-photon collisions depends on the starting point $\bar{r}_o$.)

Now, by separating $\bar{E}'$ to E' and $\bar{\omega}'$, taking into account (3.18) and using the same track-length type quality ℓ as introduced by (3.19) and interpreted at the source contribution:

$$\lambda' = \iint d\bar{r} d\bar{E} \hat{\chi}(\bar{r},\bar{E}) \frac{1}{4\pi} \hat{C}_E(E_o,E|\bar{r}) \int d\tau \ell[\bar{r},E_o,\bar{\omega}'(\bar{\omega},\cos\vartheta^*,\tau)],$$

where τ is the azimuth of the scattering and

$$\cos\vartheta^* = g(E_o,E).$$

The integration for τ can be replaced by an inner Monte Carlo procedure: an azimuth is selected randomly from $(0; 2\pi)$ and $\bar{\omega}'$ is determined so that

$$\bar{\omega}\bar{\omega}' = \cos\vartheta^*.$$

By this method the score of a collision to the flux is estimated before each pseudo-collision:

$$s = w_\chi \hat{C}_E(E_o, E_\chi | \bar{r})\, \ell(\bar{r}, E_o, \bar{\omega}'), \qquad (3.20)$$

assuming that the points $(\bar{r}, E_\chi, w_\chi)$ of all collisions and all simulations give a good representation of the $\chi(\bar{r},\bar{E})$ distribution. E_χ denotes the pseudo-photon's energy and w_χ its weight - both before the collision event. The $\hat{C}_E(E_o, E_\chi | \bar{r})$ quantity is proportional to the probability that a particle having an energy of E_χ will be scattered by the pseudo-collision to the vicinity of the source energy: $E_o \pm dE_o$.

If there is more than one source region, the total score is a sum of the scores obtained for the different regions.

3.2.5 Scores for more than one source energy line

If there is more than one type of source the contributions of the uncollided particles are calculated separately for each source type. If one source type has more than one energy line, then the different pseudo-photon energies (E_o-s of (3.18)) are selected with probabilities proportional to the intensities of the lines.

In the scattering simulation processes the contributions to all lines of all source types are calculated before each collision (*Fig. 12*). Naturally there is no contribution to the lines whose energies (E_o) are less than that of the pseudo-photon (E), or if

$$E < \tfrac{1}{2}\varepsilon \quad \text{and} \quad E_o > \frac{E}{1 - 2\,\frac{E}{\varepsilon}},$$

where $\varepsilon = m_e c^2 \approx 511$ keV, (see Subsection 3.4.2).

This simultaneous technique reduces the computation time since the time-consuming random walk processes are simulated only once for all source types. Hence, it is suggested to combine calculations for different sources into a single task, even if they are separate cases in physical reality. Nevertheless, if the highest energy of one (or more) of the source types lies much lower than the maximum energy concerned in the whole problem, then most pseudo-photons will start even with energies exceeding this highest energy and therefore the scoring events for such sources will be rare, i.e. the results obtained for such source types will have very large statistical uncertainties.

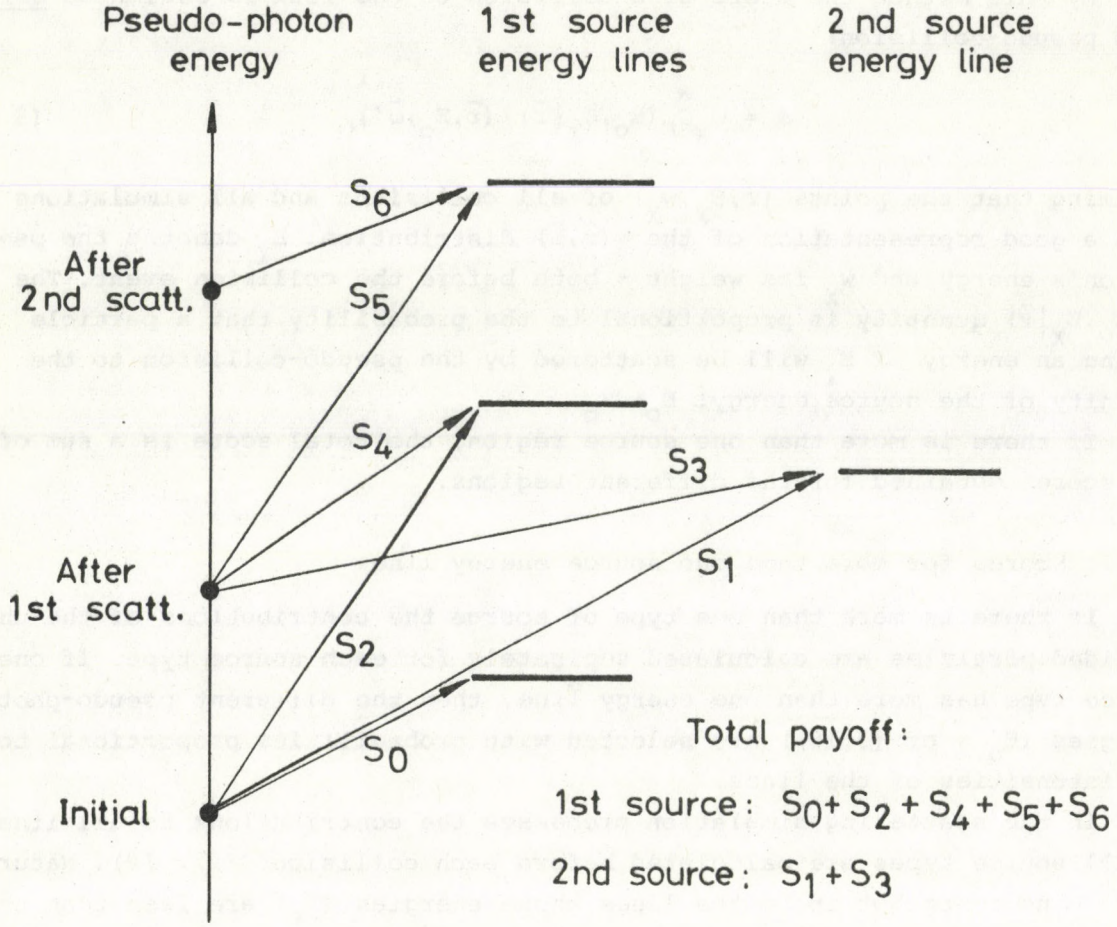

Fig.12. Simultaneous calculation of the contributions to all energy lines

3.3 DOSE CALCULATIONS

As in most low energy photon dose calculations only interactions of the photons are followed, i.e. the energies of the secondary charged particles are assumed to be deposited at the sites of their creation. In other words it means that we approximate the absorbed dose by the kerma. This approximation is quite reasonable for energies below about 3 MeV.

The connection between the fluence rate and dose rate is given by

$$\dot{D} \simeq \dot{K} = \frac{\mu_k(E)}{\rho} E \varphi, \qquad (3.21)$$

therefore the initial statistical weight of the pseudo-particles is multiplied by

$$\frac{\mu_k(E)}{\rho} E$$

for the dose rate calculation.

In ORNL phantoms three regions having different types of tissues are specified: the skeleton, the lungs and the remainder of the body (soft tissue). For our task there is only one problematic point with this phantom: that relating to the bone marrow, since there is no geometrically separated marrow region in the phantom. The marrow dose in most earlier Monte Carlo calculations with this phantom was estimated simply by taking the weight proportional fraction of the bone doses. Now, in our adjoint model this method has been modified in such a way that while the bone is still considered to be a homogeneous medium during the random walk simulation of the pseudo-photons, at the flux to kerma rate conversion (3.21) the mass energy transfer coefficients (μ_k/ρ) are calculated for the real bone marrow material - taken after the "reference man" of ICRP [11] as given in Table V.

Table V Compositions of the red and yellow marrows. (The most important elements of the ICRP reference man are taken.)

Element	Weight per cent	
	red marrow	yellow marrow
H	10.43	11.50
C	43.09	64.25
N	3.34	0.65
O	43.09	23.00
Na	0.05	0.41
P	-	0.01
S	-	0.07
Cl	-	0.11

3.4 CROSS SECTION HANDLING

In the calculation of the total linear attenuation coefficient (μ) only the two major types of interactions are taken into account:

$$\mu = \mu_{pe} + \mu_c^{KN}$$

where μ_{pe} is the linear attenuation coefficient of the photoelectric absorption

and μ_c is that for the Compton effect, as described by the Klein-Nishina formula.

Pair-production, occurring only above $2m_e c^2 \simeq 1022$ keV and having low cross sections below 3 MeV, as well as coherent-scattering, having a remarkable effect only at very small energies, are neglected.

In the flux to kerma rate conversion the

$$\mu_k = \mu_{pe} + \mu_{tr}^{KN}$$

relation is used, where

μ_{tr} is the energy transfer coefficient, again calculated on the basis of the Klein-Nishina formula.

3.4.1 Library for the photoelectric cross sections

The photoelectric cross sections for all 92 natural elements and for the 5 keV - 3 MeV range are stored in a built-in library. The library data are taken from the Lawrence Livermore Laboratory Library [12].

The photoelectric cross section vs. energy curves are more-or-less straight lines in log-log plots for most elements, therefore log-log interpolations are used between any two base points. There are seven "standard" base points at 5, 15, 40, 100, 250, 1000 and 3000 keV and the cross section pairs (see *Fig. 13*) at every absorption edge are also tabulated. (There is no edge above 5 keV for the first 22 elements; at the end of the list, uranium has as many as six edges).

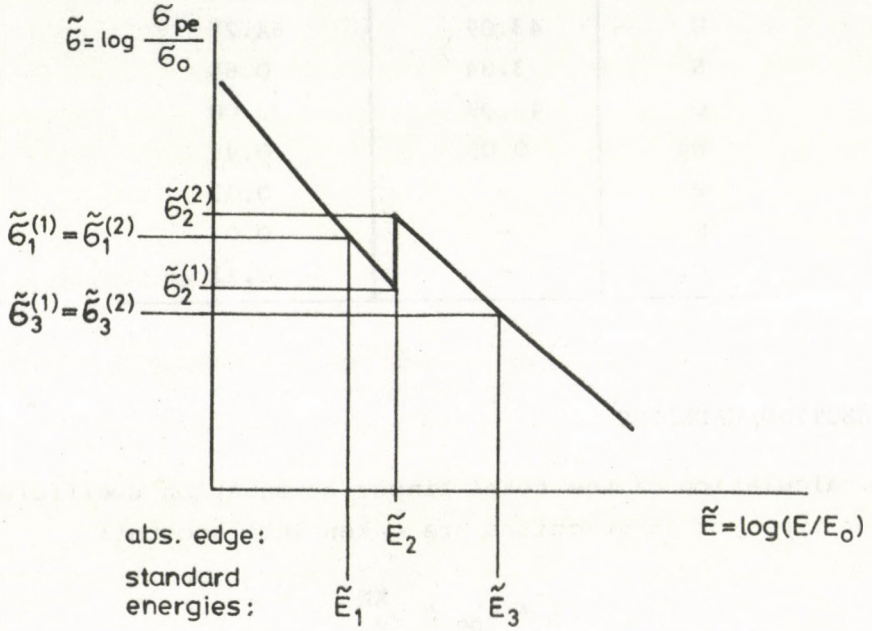

Fig. 13. Illustration of the structure of the photoelectric library

In the actual library the logarithms of the standard energies, the edge energies and the cross sections are stored. The bases E_o and μ_o in *Fig. 13* are 1 keV and 1 barn, respectively.

3.4.2 Calculation of the Compton cross sections

As mentioned earlier the Compton scattering events are always approximated by the Klein-Nishina formula, i.e. we neglect the electron binding effect. This approximation leads to a slight overestimation. The error caused by omitting the coherent scattering is opposite in sign and the total error resulting from these two simplifications is practically always less than 10 per cent of the total cross section [13].

The energy change function f_E of (3.4) described by the Klein-Nishina cross section for one element is:

$$f_E(E \to E') = \frac{N_A \rho}{A} z \sigma_c^1$$

where N_A is Avogadro's constant (6.022×10^{23});

z is the atomic number,

A is the atomic weight of the element,

ρ is the density,

and σ_c^1 is the Compton cross section of one electron:

$$\sigma_c^1 = \frac{r_o^2}{2} f^*(E,E') = \frac{r_o^2}{2} \frac{\varepsilon}{E^2} \left[\frac{E'}{E} + \frac{E}{E'} + \left(1 + \frac{\varepsilon}{E} - \frac{\varepsilon}{E'}\right)^2 - 1 \right], \qquad (3.22)$$

where r_o is the classical electron radius (2.818×10^{-13} cm),

$\varepsilon = m_e c^2 \simeq 511$ keV is the rest mass energy of the electron,

and

$$\frac{E}{1+2\frac{E}{\varepsilon}} < E' < E.$$

The total Klein-Nishina cross section can be expressed analytically by the integration of the differential form but the exact formula has some disadvantages for computation (slow-to-evaluate logarithms and near cancellation of terms), therefore, instead, the empirical fit given by Hastings [14] is used:

$$\sigma_c^1 \simeq \pi r_o^2 \frac{A\alpha^2 + B\alpha + C}{\alpha^3 + D\alpha^2 + E\alpha + F}, \qquad (3.23)$$

where α is the photon energy in electron rest mass energy ($\varepsilon = m_e c^2 \simeq 511$ keV) units, $\alpha = E/\varepsilon$,

$A = 7.435855$, $D = 69.814184$,

$B = 256.433669$, $E = 279.962207$,

$C = 243.570663$, $F = 91.353238$.

The exact formula of the energy transfer cross section suffers from the same type of numerical problems so we have developed an approximate expression of it [15]:

$$\sigma_{tr}^{1} \simeq \pi r_o^2 \frac{P\alpha+Q\alpha^2}{1+R\alpha+S\alpha^2+T\alpha^3}, \tag{3.24}$$

where $P = 2.676912$,
$Q = 1.808298$,
$R = 5.081739$,
$S = 4.763744$,
$T = 0.478992$.

The errors of the two fits are less than 0.2 and 0.4 per cent, respectively, in the $0<E<3$ MeV range.

3.4.3 Cross sections of compounds

The total attenuation coefficient of a compound consisting of m elements with weight proportions of w_i /i = 1,2,..,m/ is

$$\frac{\mu}{\rho} = \sum_i w_i \left(\frac{\mu}{\rho}\right)_i . \tag{3.25}$$

The individual attenuation coefficients for the elements can be calculated from the cross sections by

$$\left(\frac{\mu}{\rho}\right)_i = \sigma_i \frac{N_A}{A_i}, \tag{3.26}$$

where N_A is Avogadro's number and A_i is the atomic weight.

The

$$C_i = \frac{N_A}{A_i} \times 10^{-24} \tag{3.27}$$

values are stored in the cross section library for all 92 elements, the 10^{-24} factor converts the cross section from barn to cm^2.

The evaluation of the photoelectric cross section is carried out as indicated by (3.25) and (3.26). If there are more elemenents with absorption edges in the investigated energy range, then the compound's base points will comprise all of them, and the photoelectric cross section pairs (below and above the edge energy) will be computed and summarized for all elements at every edge. The standard base energies are also included among the final base points but if there is an edge energy in the 20 per cent vicinity, then the standard energy is omitted. Naturally, the two cross section values at a standard point are equal to each other (*Fig. 14*).

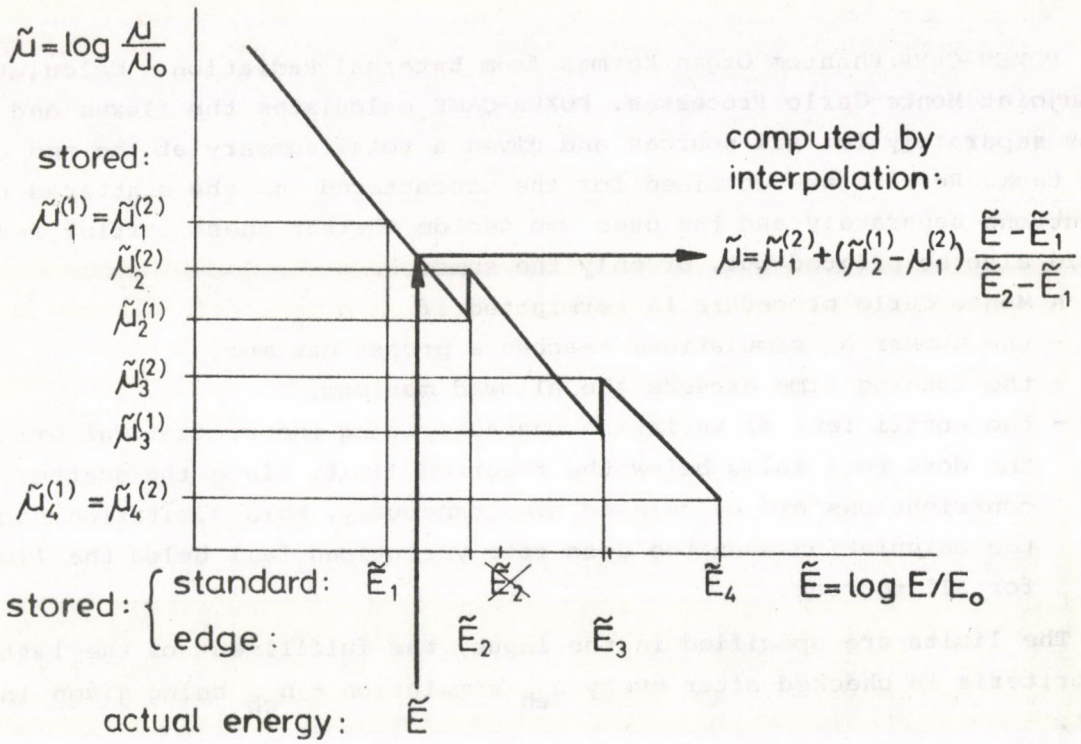

Fig.14. Photoelectric cross section calculation
(E_o = 1 keV, μ_o = 1 cm^{-1})

The total Compton cross section of an element with atomic number z_i is

$$\sigma_c = z_i \sigma_c^1, \tag{3.28}$$

where σ_c^1, the cross section of one electron as given by (3.22), is independent of the element, therefore the Compton mass attenuation coefficient μ_c/ρ of a compound can be calculated from (3.25), (3.26) and (3.27) as

$$\left(\frac{\mu}{\rho}\right)_c = \sigma_c^1 \sum_i w_i \frac{N_A}{M_i} z_i,$$

where the weighted average of the atomic number

$$z_{av} = \sum_i w_i N_A \frac{z_i}{M_i} \tag{3.29}$$

is calculated for each material at the beginning of the task. The z_i/M_i ratios are stored in the cross section library for all the elements.

For the air and the human tissues the photoelectric cross section interpolation table and the z_{av} values are directly built into the code.

4. USER'S MANUAL

POKER-CAMP: Phantom Organ Kermas from External Radiation - Calculation by Adjoint Monte-Carlo Processes. POKER-CAMP calculates the fluxes and dose rates separately for all sources and gives a total summary at the end of each task. Results are obtained for the unscattered and the scattered contributions separately and the user can decide whether these partial results should also be printed out, or only the sums.

A Monte Carlo procedure is terminated if

- the number of simulations reaches a preset maximum,
- the running time exceeds the allowed maximum,
- the coefficient of variation characterizing the statistical error of the dose rate falls below the required limit. Since the scattered contributions are calculated simultaneously, this limitation stops the calculation when the dose rate variations fall below the limit for all sources.

The limits are specified in the input, the fulfillment of the latter two criteria is checked after every n_{ch} simulation - n_{ch} being given in the input.

The user can file any number of tasks in a single run.

POKER-CAMP is written in FORTRAN-IV. The core required on the R-40 computer (product of GDR, similar to IBM 360) of the Central Research Institute for Physics is 280 Kbyte.

The following special subroutines are used:

RANDU(IX, IY, IF) - random number generator of the IBM Scientific Subroutines Package.

TIMEL(T) - clock, T is the cpu time in seconds (8 byte real variable) elapsed from the last call of TIMEL or TIMSET.

TIMSET - sets time to zero at the beginning.

4.1 INPUT OF THE CODE

Card A (2I5)

KINDO - general specification of the taks:

= 0: there is no more task, the run is ended
= - 1: the gamma library is to be printed out
= - 2: the cross section library is to be printed out
= 1: calculations for a free-in-air detector point
= 2: a point detector is placed on the male phantom
= 3: a cylindrical detector is studied
= 4: a spherical phantom is studied
= 5: doses in the male phantom are calculated
= 6: doses in the female phantom are calculated
= 7: the effective dose equivalent is calculated

If KINDO = -1, or -2, then KD has no meaning, and no more input data are needed.

KD - its meaning depends on KINDO:

if KINDO = 1, or 2:

= 0: only the air kerma rate is calculated

= N: N special detector responses are calculated (N≤10)

if KINDO = 3:

= 1: the cylindrical detector is bare

= 2: the cylindrical detector is covered

if KINDO = 4:

= 1: the dose rate for the whole sphere is calculated

= 2: a selected point in the sphere is considered

if KINDO = 5, or 6: KD specifies the target organ:

= 1: whole body

= 2: testicles (for male phantom only)

= 3: ovaries (for female phantom only)

= 4: red (or active) bone marrow

= 5: yellow bone marrow

= 6: lungs

= 7: thyroid lobes

= 8: breasts (for female phantom only)

if KINDO = 7: KD has no meaning

Card B (F10.3)

ELOW - the low energy limit [in keV], suggested range: 10-20 keV, the minimum (due to the cross section tabulations) is 5 keV.

Card C (F10.3): only if KINDO = 1,2,3, or 4:

DEZ - if KINDO = 1: the position of the point-like detector (z_D in *Fig. 4*) [in cm]

if KINDO = 2: the position of the point detector on the phantom's chest (in phantom coordinates, z'_D in *Fig. 4*) [in cm]

if KINDO = 3, or 4: the position of the detector centre (z_D in *Figs. 6 and 7*)

= = = = = = = = =

Card set D - only for point detectors: (if KINDO = 1, or 2) and KD ≠ 0. In such cases KD sets of cards D specify the special detectors.

Card $D1_K$(2(A8,2X),4I5): specification of detector K:

TXR(K) - a max. 8 character name of the detector

TXU(K) - a max. 8 character name of the unit of the detector reading

KRES(K) - if>0 : the response of the detector is calculated from the flux
if<0 : the response is calculated from the kerma rate
|KRES(K)| = 1: the energy and angular sensitivities can be separated
|KRES(K)| = 2: a sensitivity matrix is given below

NER(K) - the number of the energy base points ($\leq$30), set 0, if the response is energy independent

NAR(K) - the number of the angle base points ($\leq$30),set 0, if the response is independent of the angle of incidence

IANG(K) - the angles are measured from the
= 1: positive z axis
= 2: positive y axis
IANG(K) has no meaning if NAR(K) = 0

- - - - - - -

If|KRES(K)|= 1, continue by cards D2 and D3,
if|KRES(K)|= 2, continue by cards D4, D5 and D6.

- - - - - - -

Cards $D2_{K,I}$(2F10.3): NER(K) cards D2 are used for each detector, no card D2 is needed if NER(K) = 0.

ERP(K,I) - the I-th energy base point [in keV], ERP(K,I)>ERP(K,I-1)
ERV(K,I) - the sensitivity of the detector at the I-th energy [the unit is specified on card $D1_K$]

Cards $D3_{K,J}$(2F10.3):NAR(K) cards D3 are used for each detector, no card D3 is needed if NAR(K) = 0.

ARP(K,J) - the J-th angle base point [in degrees], ARP(K,J)>ARP(K,J-1)
ARV(K,J) - the sensitivity of the detector at the J-th angle [the unit is specified on card $D1_K$]

- - - - - - -

Card(s) D_4(7F10.3)
ERP(K,I), I=1,NER(K) - the energy points of the response matrix [in keV], ERP(K,I)>ERP(K,I-1)

Card(s) D_5(7F10.3)
ARP(K,J),J=1,NAR(K) - the angle points of the response matrix [in degrees], ARP(K,J)>ARP(K,J-1)

Cards D_6(7F10.3): separate cards D_6 must be given for all energy points (I=1,NER(K))

RMX(K,I,J),J=1,NAR(K) - the sensitivity of the K-th detector on the I-th energy and J-th angle of incidence [the unit is specified on card D_1]

= = = = = =

Card set E - only for the cylindrical detector (if KINDO = 3)

Card E1(I5,3F10.3)

LMNT - the number of elements in the detector material ($\leq$10)

RHO - the density of the detector material [in g/cm^3]

RDET - the radius of the cylindrical detector (r in *Fig. 6*) [in cm]

HDET - the height of the detector (h in *Fig. 6*)[in cm]

Cards E2(I5,F10.3): as many as LMNT cards E2 specify the composition of the detector material

ID(LM) - the atomic number of the LM-th component

PERC(LM) - the weight fraction of the LM-th component [in %]

Card E3(I5,3F10.3): specification of the cover. Use this card and card E4 if the detector is covered, omit them if KD = 1

LMNT - the number of elements in the detector cover ($\leq$10)

RHO - the density of the cover [in g/cm^3]

RCOV - the outer radius of the cover (r_c in *Fig. 6*) [in cm]

HCOV - the height of the cover (h_c in *Fig. 6*) [in cm]

Cards E4 - the same type of data in the same format as cards E2 but for the covering material

= = = = = =

Card set F - only for the spherical phantom (if KINDO = 4)

Card F1(I5,2F10.3)

LMNT - the number of elements in the sphere ($\leq$10)

RHO - the density of the sphere [in g/cm^3]

RDET - the radius of the sphere (r in *Fig. 7*) [in cm]

Cards F2 - the same type of data in the same format as cards E2, but for the spherical phantom

Card F3(2F10.3): this card is used only if KD = 2, to specify the place of the point investigated inside the sphere:

XSP - the x coordinate in phantom coordinate system (x_1' in *Fig. 7*) [in cm]

ZSP - the z coordinate in phantom coordinate system (z_1' in *Fig. 7*) [in cm]

= = = = = =

Card G(F10.3)

THICK - the thickness of the intermediate layer (t in *Fig. 1*) [in cm]. Set 0, if there is no intermediate layer

Card set H - specifies the intermediate layer material. Omit these cards if there is no layer (THICK = 0.)

Card H1(I5,F10.3)

LMNT - the number of elements composing the layer material ($\leq$10)

RHO - the density of the layer material [g/cm^3]

Cards H2 - the same type of data in the same format as cards E2, but for the layer material

= = = = = =

Card set J - specifies the composition of the soil

Card J1 } the same type of data in the same format as cards H1
Cards J2 } and H2, respectively, but for the soil material

= = = = = =

Card K(I5)

NSOUR - the number of sources present in one task ($\leq$10)

As many as NSOUR sets L specify the sources:

Card L1(A8,2X,I5)

TX5(I) - the name of the I-th source

NE(I) - the number of the energy lines in the spectrum of the I-th source. If NE(I) = 0, then the spectrum is taken from the built-in gamma line library, therefore in such cases TX5(I) must be identical with one of the "Identification word"-s of Table I.

Cards L2(2F10.3) - specify the gamma energies and their intensities; if not, the catalogue is used, i.e. if NE(I) ≠ 0. As many as NE(I) cards L2 are used for the I-th source.

EL(I,J) - the energy of the J-th line [in keV], EL(I,J)>EL(I,J-1)

ELIN(I,J) - the absolute intensity of the J-th energy line [occurrence per cent of disintegrations]

Cards L3(I5,2F10.3): there are three cards L3 for the regions:

J = 1: air
= 2: intermediate layer
= 3: soil bulk

KS(I,J) - the geometrical distribution of the I-th source in the J-th region:
= 0: there is no source in the J-th region (zero must be given in the second card if there is no intermediate layer)
= 1: the source is uniformly distributed
= 2: the source intensity is exponentially decreasing with the depth in the solid layers, or with the height in the air
= 3: a plane source is considered

ACT(I,J) - the activity of the source (S_i in *Fig. 2*), the maximum activity in the exponential case. The unit is [Bq/cm^3] if the distribution is uniform or exponential, and [Bq/cm^2] if a plane source is specified

PAR(I,J) - has no meaning if the source is uniformly distributed,
- is the relaxation length (ζ_i in *Fig. 2*) [in cm] if the distribution is exponential
- is the place of the plane source if it is in the air (h in *Fig. 2*) [in cm]. It has no meaning if plane source is defined on top of a solid region.

= = = = = =

Card M(3I5)

NENG - the number of energy groups, if spectra are also to be calculated. Zero indicates that spectra differential by energy are not to be calculated

NANG - the number of the angular groups. Zero indicates that spectra differential by the angle of incidence are not to be calculated

KANG - the angles, for the spectrum determination, are measured from
= 1: the positive z axis
= 2: the positive y axis

Card N1(2I5, 2F10.3)

NPH - the maximum number of simulations for the calculation of each uncollided source contribution

NCH - the number of simulations after which the error and running time checks are carried out in the source contribution calculations

TLIM - the cpu time limit for the calculation of the uncollided contribution of one source [in s]

ERR - the error limit [in %]. If the coefficient of variation of the dose rate for the uncollided contribution falls below this limit, there are no more simulations

Card N2(2I5, 2F10.3)

NPHA, NCHA, TLIMA, ERRA } The same types of quantities as on card N1 but for the simultaneous calculation of the scattered contributions from all sources. The error criterion must be fulfilled for the dose rates for all sources.

Card P(I5): controls the print out of the results:

IPR = 0: only the total values (uncollided + scattered) are printed out for all sources

= 1: the contributions of the uncollided photons and the total values are printed out

= 2: the contributions of the uncollided and the scattered contributions as well as total values are printed out

= = = = = =

The reading of the input data is repeated from card A, for the specification of the next task of the run.

* * *

A sample input is given in the Appendix

4.2 OUTPUT OF THE CODE

The print out is controlled in the following way: the number of lines still empty on the page currently used is compared with the number of lines needed for the next series of closely-related data. If the room on the current page is not enough for printing a coherent set of data, a new page is opened.

For all tasks, the execution starts with a print out of all physical input data.

The results are printed out for every source separately and finally a total summary is given, where the fluxes and doses are summed for all sources.

If the partial results are also printed out, they are identified by the words

"uncollided part"

and "scattered part",

while their sums are marked as

"total values".

Moreover, the cpu times and - with the prints of the partial results only - the numbers of simulations are given.

The units are given with all quantities and SI units are used - except if the user specifies other units for the readings of the special detectors.

* * *

A sample output is given in the Appendix.

4.2.1 Notes on the statistical uncertainties

The statistical uncertainty, an unavoidable consequence of the application of the Monte Carlo technique, is characterized by the coefficient of variation. Therefore it is printed with every result, generally in parentheses.

The variances of simple averages ($\bar{x}$): the <u>flux</u> or <u>dose rate</u> values are calculated by the well-known empirical formula (N>>1):

$$\sigma^2 = \frac{1}{N^2}\left[\Sigma x_i^2 - \frac{(\Sigma x_i)^2}{N}\right]$$

where x_i denotes the contribution of the i-th particle (i=1, 2,...,N). (Naturally the contributions obtained during different collisions of the same particle are simply summed before the calculation of the variance.)

The coefficient of variation is:

$$CV = 100\,\frac{\sigma}{\bar{x}} = 100\sqrt{\frac{\Sigma x_i^2}{(\Sigma x_i)^2} - \frac{1}{N}} \quad [\%]. \qquad (4.1)$$

This formula is used in the calculations of both the uncollided and the scattered parts. When the two contributions are summed for the total ($x = x_u + x_s$), the variance is calculated by

$$\sigma^2 = \sigma_u^2 + \sigma_s^2,$$

as the two results are statistically independent of each other. Similarly, when the flux or the kerma rate /X/ is calculated for the total summary

$$X = \Sigma X_i,$$

where X denotes the total sum,

X_i is the contribution from the i-th source, then the over-all error is estimated similarly, as

$$\sigma_X^2 = \sum_i \sigma_{X_i}^2 ,$$

though it must be noted here that this calculation of the resultant coefficient of variation is not fully correct since the scattered contributions for the different sources are simultaneously calculated from the same histories, i.e. the scattered parts of the results are not independent of each other.

In the calculation of the average energy the formula

$$\bar{E} = \frac{\Sigma \varphi_i E_i}{\Sigma \varphi_i}$$

is used, where E_i is the i-th pseudo-photon's energy and φ_i is its contribution for the uncollided or the scattered part. Here the numerator and the denominator terms are correlated. The variance is (as derived in [16]):

$$\sigma^2 = \frac{\Sigma (\varphi_i E_i)^2 + \frac{\Sigma (\varphi_i E_i)^2}{(\Sigma \varphi_i)^2} \Sigma \varphi_i^2 - 2 \frac{\Sigma \varphi_i E_i}{\Sigma \varphi_i} \Sigma \varphi_i^2 E_i}{(\Sigma \varphi_i)^2} \qquad (4.2)$$

The average energy of <u>all photons</u> is defined by

$$\bar{E} = \frac{\frac{1}{N} \Sigma \varphi_i e_i + \frac{1}{M} \Sigma \psi_j \varepsilon_j}{\frac{1}{N} \Sigma \varphi_i + \frac{1}{M} \Sigma \psi_j}$$

where φ_i-s (i = 1,2,...,N) are the flux contributions of the uncollided photons having energies e_i, and ψ_j-s (j = 1,2,...,M) are the flux contributions of the pseudo-photons starting with ε_j energy. In this case the varience is:

$$\sigma^2 = \frac{1}{(\frac{1}{N} \Sigma \varphi_i + \frac{1}{M} \Sigma \psi_j)^2}$$

$$\times \{ \frac{1}{N^2} \left[\Sigma (\varphi_i e_i)^2 - \frac{(\Sigma \varphi_i e_i)^2}{N} + \bar{E}^2 (\Sigma \varphi_i^2 - \frac{(\Sigma \varphi_i)^2}{N}) - 2\bar{E} (\Sigma \varphi_i^2 e_i - \frac{\Sigma \varphi_i e_i \Sigma \varphi_i}{N}) \right]$$

$$+ \frac{1}{M^2} \left[\Sigma (\psi_j \varepsilon_j)^2 - \frac{(\Sigma \psi_j \varepsilon_j)^2}{M} + \bar{E}^2 (\Sigma \psi_j^2 - \frac{(\Sigma \psi_j)^2}{M}) - 2\bar{E} (\Sigma \psi_j^2 \varepsilon_j - \frac{\Sigma \psi_j \varepsilon_j \Sigma \psi_j}{M}) \right] \} .$$

4.3 SEGMENTS OF THE CODE

The segments are listed below, in the same alphabetical order as in the program list, together with several words concerning their roles. This information is of help if the user intends to make any kind of modification in the code.

MAIN - controls the whole program operation.

FUNCTION ALPHA(K,E) - gives the sensitivity of the K-th detector to energy E, if the energy dependence of that detector is separable. The value ALPHA is equivalent ot α or α^* of (2.5) or (2.6).

FUNCTION BETA(K,A) - calculates the sensitivity of the K-th detector for the angle of incidence A, if the angular dependence of that detector is separable. Angle A is given in [rad], BETA is equivalent to β or β^* of (2.5) or (2.6).

FUNCTION CP(I,A) - gives the Compton mass energy transfer coefficient according to the approximate formula (3.24) for the I-th material on the energy $A = E/m_e c^2$.
The materials are numbered as:
I = 1: air,
= 2: layer,
= 3: soil,
= 4: cylindrical detector or spherical phantom,
= 5: cover of the cylindrical detector,
= 6: bone tissue,
= 7: lung tissue,
= 8: soft tissue,
= 9: red bone marrow,
=10: yellow bone marrow.

FUNCTION CV(X,X2) - calculates the coefficient of variation as given in (4.1), X represents Σx_i, X2 denotes Σx_i^2.

FUNCTION EXPSP(A) - replaces the standard function EXP(A), to avoid underflow errors if A is a too large negative number.

FUNCTION GAMM(K,E,A) - determines the response of the K-th detector on energy E and angle of incidence A. GAMM is equivalent to γ or γ^* in (2.1) or (2.2). A is the angle ϑ of (2.1) and (2.2) - in [rad].

FUNCTION GAM2(K,L,A) - calculates the equivalent to γ or γ^* as above, but for the L-th source line. This routine is used in the uncollided contribution calculation since in

that case there are only the discrete source energies where the sensitivities are to be calculated. The interpolation is based on V2(K,L,J), where J is the J-th angle base point. Elemenets of V2 are created by SUBROUTINE GAM1.

FUNCTION HP(I,A) - gives the Compton mass attenuation coefficient according to the Hastings approximation (3.23). For explanations of I and A, see Function CP.

FUNCTION PHEL(I,E) - calculates the linear photoelectric attenuation coefficient by interpolation as illustrated in *Fig. 13*. The meaning of I is the same as in Function CP. E is the energy in [keV].

BLOCK DATA - stores the weighted atomic numbers (ZAV), the densities (RHO), numbers of base points for the photoelectric cross section interpolation (NBRK), the base energies (EBRK) and the photoelectric cross section pairs (SP1 and SP2) for the air and the five phantom tissues (See *Fig. 13*).

FUNCTION UPINT(A,K) - determines the (3.11) integral for the K-th material on energy $A = E/m_e c^2$.

SUBROUTINE ATTEN(A,K,KON)- calculates the total attenuation coefficients (ST) and the flux-to-kerma-rate conversion factors (DC). The variable IAC(I) governs whether for material I (as listed by Function CP)

IAC(I) = 1: only the cross section,
= 2: both the cross section and the conversion factor,
= 3: only the conversion factor

to be calculated.

IAC(I) = 0 indicates that there is no material I in the task.

If KON = 0, there is no conversion factor calculation at all.

SUBROUTINE BREQ(J) - determines the crossing point of a line with a breast ellipsoid of the female phantom. The calculation is carried out for

J = 1: the left breast,
= -1: the right breast.

B-D is the distance to the entering and B+D to the outgoing point.

SUBROUTINE CONEQ(J) - carries out similar calculations for the two leg cones of any phantom.

SUBRØUTINE CØSEQ(I) - calculates similarly crossing points with
I = 1: the upper part of the head,
= 2: the lower part of the head + the neck,
= 3: outer covering cylinder of the male phantom,,
= 4: outer covering cylinder of the female phantom.

SUBRØUTINE CRØCY - determines the crossing points with the cylindrical detector,
ICR = 0: there is no crossing,
1: there is one crossing,
2: there are two crossings, the path starts from the detector and goes through the cover,
3: there are three crossings, the path goes once through the detector and twice through the cover.
The distances to the J-th entrance and exit points are TI(J) and TØ(J), respectively (J = 1,..,ICR), if ICR ≠ 0.

SUBRØUTINE CRØCY2(K,R2,H2,H2S) - calculates the crossing points with a cylindrical box. This is an auxiliary routine to CRØCY. R2 is the square of the cylinder radius, H2 is the half height of the cylinder, and H2S is the product of H2 with the sign of the z component of the pseudo-particle's direction of flight.
K = 0: if there is no crossing,
= 1: if the path crosses the box.

SUBRØUTINE CRØPH - determines the crossing points of the pseudo-photon with a human phantom.
ICR is the number of crosses since the path can enter and leave the phantom more than once. TI and TØ elements have the same meaning as in Subroutine CRØCY.

SUBROUTINE CRØSP - determines the crossing points with the spherical phantoms. The meaning of ICR (0, or 1) and TI and TØ are the same as in Subroutine CRØCY.

SUBRØUTINE CRPREP(I) - prepares the base point values for the photoelectric cross section interpolations - for material I.
It works from the built-in library.

SUBRØUTINE EDITCR - prints out the content of the cross section library, if the code is run by KINDO = -2.

BLOCK DATA - stores the following cross section /or similar/ data:

ENERGY - logarithms of the standard energies, (i.e. of the figures if the unit is [keV]),

CONV - conversion factors for the 92 elements, that convert the photoelectric cross section from barn/atom to g/cm^2,

ZALM - atomic number/atomic weight ratios for the 92 elements,

IDRF - the register shift for the 92 elements. For a given chemical element it means that data are given from the (IDRF+1)-st element of CRS,

CRS - the block of all cross sections. For each element the first 7 items are the cross sections (i.e. logarithms of the figures of the photoelectric cross sections, if the unit is barn), then - for the elements with atomic numbers exceeding 22 - the number of edges is specified, then the edge energies and the cross section pairs are given, in the same logarithmic manner as mentioned above.

The standard energies are in increasing order; the edges are ordered in the opposite way, i.e. starting from the highest energy.

SUBROUTINE EDITGL - prints out the content of the gamma lines library, if the code is run by KINDO = -1.

BLOCK DATA - stores the following library data:

IDENT - the maximum 8 character identification words (see Table I),

IDR - register shift for the 40 sources (as in the cross section library),

ENGL - the energies of the lines [in keV],

AIGL - the corresponding absolute intensities [in %].

SUBROUTINE GAM1(K,L,E) - prepares the V2(K,L,J) elements, by interpolation from the RMX matrix-elements (the $m_{i,j}$ elements in (2.2) and (2.4)) for the source energies.

SUBROUTINE GOON - selects the new collision site by the methods described in Subsection 3.2.2.

SUBROUTINE INITL - directs the whole calculation of the uncollided contributions. The total attenuation coefficients at the source energies, that are frequently used

in the scattered part calculations, too, are determined first and stored in STL.

SUBROUTINE INPUT - reads in the input data and modifies them as necessary for the other routines.

SUBROUTINE INSOUR(F,KEN,J) - calculates the track length type quantity ℓ of (3.19).
F is the track length type quantity for the J-th energy line of the KEN-th source.

SUBROUTINE LINES - selects the lines of the different sources from the built-in gamma catalogue.

SUBROUTINE NEWCOS - selects the new direction cosines of the pseudo-photons after each collision.
DX, DY and DZ are the compnents of the $\bar{\omega}$ vector, DXY = SQRT(1. - DZ*DZ).

SUBROUTINE OUTPUT - directs the print out of all results.

SUBROUTINE PATHS(KEN) - determines the distances that the pseudo-particle should fly to reach several horizontal planes:
RO - is the distance to the z = 0 plane,
RTH is the distance to the z = -t plane, i.e. to the plane separating the layer and the soil bulk,
RAIR is the distance to the z = h plane, the height of the plane source in the air for the KEN-th source. RAIR is calculated only if KS (KEN,1) = 3.
If KEN is set to zero, RAIR is not calculated at all.

SUBROUTINE PAYOFF(A,E) - calculates the pay-off for the scattered part, as given by (3.20). The $\hat{C}_E$ factor is represented by symbol P in the program, the track length part is taken from Subroutine INSOUR. A and E are the energies in $m_e c^2$ and keV units, respectively.

SUBROUTINE SCATUP(A,CPSI,SPSI)- selects the pseudo-photon's energy and the angle of scattering for the pseudo-collisions by the method described in [10]. It also modifies the statistical weight as mentioned in Subsection 3.2.4.
A is the energy in $m_e c^2$ units (before collision as input value, and after collision as output value).
CPSI and SPSI are the cosine and the sine of the scattering angle, respectively.

SUBROUTINE SELECT - selects the initial coordinates of the pseudo-photon with the methods described in Subsection 3.2.1. The three Cartesian coordinates are X,Y and Z. The value LL is also determined: it identifies the

material from which the pseudo-particle starts. The coding is the same as that of I in Function CP. The variable LB determines the body part from where the photon starts:

LB = 1: upper part of the head
= 2: lower part of the heat + the neck
= 3: right breast
= 4: trunk
= 5: left breast
= 6: right leg
= 7: male genitalia region
= 8: left leg.

For the cylindrical detector LB = 1 means that the point selected is in the actual detector region, 2 is given if it is in the cover.

SUBROUTINE WHERE - determines the place of a pseudo-photon in the human phantoms. LL and LB are determined, their meaning is the same as in Subroutine SELECT.

ROUTINES TO GENERATE AND TRANSFORM THE RANDOM NUMBERS

SUBROUTINE INITRD - sets the initial value of IX of the basic random number generator RANDU to 5^{13} = 1,220,703,125.

FUNCTION RDM(Q) - gives a random number from the uniform distribution on (0;1). Hereafter Q represents a dummy argument.

INTEGER FUNCTION INSRD(Q) - gives+1 or -1 with equal probabilities.

FUNCTION RDMSG(Q) - gives a random number from the uniform distribution on (-1;+1).

SUBROUTINE RDCOS2(DX,DY) - gives the direction cosines of a two dimensional random unit vector.

SUBROUTINE RDCOS3(DX,DY,DZ) - gives the direction cosines of a three dimensional random unit-vector.

REFERENCES

[1] National Bureau of Standards: Physical Aspects of Irradiation. NBS Handbook 85, Washington, D.C., 1964.

[2] U. Reus, W. Westmeyer and I. Warnecke: Gamma-ray Catalog. GSI 79-2. Gesellschaft für Schwerionenforschung, Darmstadt, 1979.

[3] International Commission on Radiation Units and Measurements: Radiation Quantities and Units. ICRU 19, Washington, D.C., 1971.

[4] W.S. Snyder, M.R. Ford, G.G. Warner and H.L. Fisher: MIRD Pamphlet No. 5, J. Nucl. Med. /Supplement No. 3/ 10, 1, 1969.

[5] W.S. Snyder, M.R. Ford, G.G. Warner and S.B. Watson: A Tabulation of Dose Equivalent per Microcurie-Day for Source and Target Organs of an Adult for Various Radionuclides. ORNL-5000, Oak Ridge National Laboratory, Oak Ridge, 1974.

[6] M. Cristy: Mathematical Phantoms Representing Children of Various Ages for Use in Estimates of Internal Dose. ORNL/NUREG/TM-367, Oak Ridge National Laboratory, Oak Ridge, 1980.

[7] International Commission on Radiological Protection: Recommendations of the ICRP. Publication 26, Pergamon Press, Oxford, 1977.

[8] D.C. Irving: Nucl. Eng. Des., 15, 273, 1971.

[9] E.J. McGrath and D.C. Irving: Techniques of Efficient Monte Carlo Simulation I-III. ORNL-RSIC-38, Oak Ridge National Laboratory, Oak Ridge, 1980.

[10] L. Koblinger: A New Energy Sampling Method for Monte Carlo Simulation of the Adjoint Photon Transport Equation. KFKI-76-57, Central Research Institute for Physics, Budapest, 1976.

[11] International Commission on Radiological Protection: Report of the Task Group on Reference Man. ICRP 23. Pergamon Press, Oxford, 1974.

[12] E.F. Plechaty, D.E. Cullen, R.J. Howerton: Tables and Graphs of Photon-Interaction Cross Sections from 0.1 keV to 100 MeV Derived from the LLL Evaluated-Nuclear-Data Library, LLL-50900, Vol. 6, Rev. 2. Lawrence Livermore Laboratory, Livermore, 1978.

[13] J.H.Hubbell: Photon Cross Sections, Attenuation Coefficients, and Energy Absorption Coefficients from 10 keV to 10 GeV. NSRDS-NBS 29, National Bureau of Standards, Washington, D.C., 1969.

[14] C.J. Hastings: Approximations for Digital Computers. Princeton University Press, Princeton, 1955.

[15] L. Koblinger: Nucl. Sci. Eng., in press.

[16] L. Koblinger: REBEL-2: An Adjoint Monte Carlo Code for the Calculation of Radiation in Dwelling Rooms. KFKI-76-65, Central Research Institute for Physics, Budapest, 1976.

[17] H.L. Beck: The Physics of Environmental Gamma Radiation Fields. In: Proc. 2nd Int. Symp. on the Natural Radiation Environment. USERDA Rep. CONF-720805-P1, 1974.

ACKNOWLEDGEMENTS

I should like to express my sincere thanks to Dr. István Fehér and Andor Andrási for their constant interest and for supporting this work. I am grateful to Andor Andrási and István Németh for their valuable comments on the report as a whole, and to Dr. Iván Lux for his comments on Chapter 3.

Thanks are due to Mrs. Magdolna Dobrocsi for drafting the figures and for typing the original manuscript. Harvey Shenker is thanked for his work of improving the English style of the report.

APPENDIX

SAMPLE PROBLEM

In the sample problem a point-like detector is placed at a height of 1 m above the ground. There is no intermediate layer. The composition and the density of the soil material are taken from Beck [17]:

component	fraction
Al_2O_3	13.5 wt%
Fe_2O_3	4.5 wt%
SiO_2	67.5 wt%
CO_2	4.5 wt%
H_2O	10.0 wt%
density:	1.6 g/cm^3

The responses of two special detectors are studied.

The first is a G-M counter covered with aluminium. The tube is put in horizontally, therefore the angles in the sensitivity matrix are measured from the +y axis of the model. The sensitivities measured by I. Németh (KFKI) are the following:

angle	0°	30°	60°	90°	120°	150°	180°
energy [keV]	sensitivity [cps/(μGy/h)]						
60	9.8	42.6	60.6	65.8	62.7	42.0	7.9
81	12.5	33.2	51.8	57.2	51.8	32.6	9.0
140	20.3	37.0	44.1	46.0	44.7	39.3	15.2
379	10.2	16.9	19.2	19.6	19.0	17.6	7.9
662	13.4	18.8	21.7	22.6	21.5	18.8	11.1
1252	19.0	21.3	24.6	26.1	25.5	24.2	15.7

The sensitivities are set to zero at 5 keV.

The other point-like detector is made of $CaSo_4$:Dy TL-powder, covered with 2 mm Al and 1 mm polyethylene. The response of this detector is set to 1 for ^{60}Co irradiations, the relative responses on other energies were measured by P.P. Szabó (KFKI) as given below:

energy [keV]	sensitivity [REL.TL/(μGy/h)]
15	6.00
38	6.57
64	6.45
91	5.06
123	2.68
180	1.46
662	1.01
1252	1.00

The most important natural sources are taken with the following activity concentrations (uniformly distributed in the soil):

Th-series	0.035 Bq/cm^3,
U-Ra-series	0.04 Bq/cm^3,
^{40}K	0.5 Bq/cm^3,

and an exponentially decreasing ^{137}Cs activity is added with a surface concentration of 0.03 Bq/cm^3 and a relaxation length of ζ = 3 cm.

The low energy limit of the simulations is taken as 15 keV. Spectra differential in energy and by angle of incidence (measured form +z) are calculated and all the results are printed out.

Sample INPUT:

```
    1    2
15,0
100,
G-M/AL      CPS              -2     7     7     2
5,          60,       81,        140,       379,       662,       1252,
0,          30,       60,        90,        120,       150,       180,
0,          0,        0,         0,         0,         0,         0,
9,8         42,6      60,6       65,8       62,7       42,        7,9
12,5        33,2      51,8       57,2       51,8       32,6       9,
20,3        37,       44,1       46,        44,7       39,3       15,2
10,2        16,9      19,2       19,6       19,        17,6       7,9
13,4        18,8      21,7       22,6       21,5       18,8       11,1
19,         21,3      24,6       26,1       25,5       24,2       15,7
CASO/AL2    REL,TL          -1     8
15,         6,0
38,         6,57
64,         6,45
91,         5,06
123,        2,68
180,        1,46
662,        1,01
1252,       1,00
0,
    6     1,6
   14    31,45
   13     7,15
    1     1,11
   26     3,15
    6     1,23
    8    55,91
    4
TH-CHAIN
    0  0,
    0  0,
    1  0,035
RA-CHAIN
    0  0,
    0  0,
    1  0,04
K-40
    0  0,
    0  0,
    1  0,5
CS-137
    0  0,
    0  0,
    2  0,03      3,
   26     8     1
10000   100         60,          2,
10000   100       1200,          2,
    2
    0
```

```
**POKER-CAMP** PROGRAM

THE KERMA RATE IS CALCULATED FOR A POINT DETECTOR          AT Z= 100.0 CM


 - A G-M/AL   DETECTOR WITH A RESPONSE GIVEN BELOW IS ALSO STUDIED.
THE CONVERSION FACTORS FORM (CPS      ) FROM (MICRO-GY/H)

ANGLE-Y(DEG):     0.0    30.0    60.0    90.0   120.0   150.0   180.0

E:   5.0 KEV      0.0     0.0     0.0     0.0     0.0     0.0     0.0
E:  60.0 KEV      9.800  42.600  60.600  65.800  62.700  42.000   7.900
E:  81.0 KEV     12.500  33.200  51.800  57.200  51.800  32.600   9.000
E: 140.0 KEV     20.300  37.000  44.100  46.000  44.700  39.300  15.200
E: 379.0 KEV     10.200  16.900  19.200  19.600  19.000  17.600   7.900
E: 662.0 KEV     13.400  18.800  21.700  22.600  21.500  18.800  11.100
E:1252.0 KEV     19.000  21.300  24.600  26.100  25.500  24.200  15.700

 - A CASO/AL2 DETECTOR WITH A RESPONSE GIVEN BELOW IS ALSO STUDIED.
THE CONVERSION FACTORS FORM (REL.TL   ) FROM (MICRO-GY/H)

  ENERGY (KEV):   15.0    38.0    64.0    91.0   123.0   180.0   662.0  1252.0
  RESP.FACTORS:  6.000   6.570   6.450   5.060   2.680   1.460   1.010   1.000

THE COMPOSITION OF THE SOIL BULK;
            DENSITY:      1.600 (G/CM3)
      ATOMIC NUMBER:       14      13       1      26       6       8
     WEIGHT PERCENT:     31.45    7.15    1.11    3.15    1.23   55.91

SOURCE NO.:  1   TH-CHAIN

  ENERGY (KEV):   39.9    58.1    96.7   136.0   208.0   238.9   282.7   335.8   409.4   462.3   510.7   582.1   724.5   782.9   856.7
  INTENSITY(%):    1.1     0.7     3.2     4.2     5.5    49.4    10.2    16.7     2.2     5.4     8.6    32.5     8.0     9.8     9.0

  ENERGY (KEV):  911.1   968.1  1146.0  1584.0  2615.0
  INTENSITY(%):   29.0    23.7     2.1    12.3    35.8

          SOURCE     SPEC. ACT.     SPEC. PAR.
           TYPE    (BQ/CM(2,3))       (CM)
   AIR       NO        0.0              0.0
 LAYER       NO        0.0              0.0
 EARTH     UNIF      3.5000E-02         0.0

SOURCE NO.:  2   RA-CHAIN

  ENERGY (KEV):   46.5    53.2   186.0   243.1   274.2   295.2   351.9   391.3   476.9   609.1   681.6   771.9   817.2   936.4  1122.0
  INTENSITY(%):    4.2     1.1     3.3     8.0     0.5    19.3    37.3     0.9     1.8    46.7     2.4     6.4     2.0     3.7    17.8

  ENERGY (KEV): 1245.0  1391.0  1530.0  1645.0  1759.0  1851.0  2119.0  2209.0  2448.0
  INTENSITY(%):    8.0     8.7     3.7     2.0    19.1     2.9     1.2     5.3     1.5

          SOURCE     SPEC. ACT.     SPEC. PAR.
           TYPE    (BQ/CM(2,3))       (CM)
   AIR       NO        0.0              0.0
 LAYER       NO        0.0              0.0
 EARTH     UNIF      4.0000E-02         0.0
```

SOURCE NO.: 3 K-40

ENERGY (KEV): 1461.0
INTENSITY(%): 10.7

	SOURCE TYPE	SPEC. ACT. (BQ/CM(2,3))	SPEC. PAR. (CM)
AIR	NO	0.0	0.0
LAYER	NO	0.0	0.0
EARTH	UNIF	5.0000E-01	0.0

SOURCE NO.: 4 CS-137

ENERGY (KEV): 661.6
INTENSITY(%): 85.1

	SOURCE TYPE	SPEC. ACT. (BQ/CM(2,3))	SPEC. PAR. (CM)
AIR	NO	0.0	0.0
LAYER	NO	0.0	0.0
EARTH	EXP.	3.0000E-02	3.0

ENERGY LIMIT: 15.0 KEV

SOURCE: IDENT.NO. 1 TYPE: TH-CHAIN UNCOLLIDED PART NUMBER OF SIMULATIONS: 3300

FLUX: 3.935E-01 (1/CM2/S) AVERAGE ENERGY: 1205.2 KEV DOSE RATE: 6.599E-03 (MICRO-GY/H)
(0.8%) (1.6%) (2.0%)

RESPONSE OF THE G-M/AL DETECTOR: 1.561E-01 CPS
(2.1%)

RESPONSE OF THE CASO/AL2 DETECTOR: 6.813E-03 REL.TL
(1.9%)

DIFFERENTIAL SPECTRA:

ENERGY: (KEV)	DIFFER. FLUX: (1/CM2/S/KEV)	C.V (%)	DIFFER. DOSE: (MICRO-GY/H/KEV)	C.V (%)
15.0- 115.0	2.520E-05	13.0	3.170E-08	13.1
115.0- 215.0	7.067E-05	9.4	1.900E-07	9.9
215.0- 315.0	5.305E-04	3.3	2.118E-06	3.3
315.0- 415.0	1.881E-04	6.5	1.094E-06	6.5
415.0- 515.0	1.757E-04	7.2	1.486E-06	7.3
515.0- 615.0	4.140E-04	4.7	4.112E-06	4.7
615.0- 715.0	0.0	100.0	0.0	100.0
715.0- 815.0	2.297E-04	7.0	2.913E-06	7.0
815.0- 915.0	5.957E-04	4.3	8.730E-06	4.3
915.0-1015.0	3.826E-04	5.6	5.979E-06	5.6
1015.0-1115.0	0.0	100.0	0.0	100.0
1115.0-1215.0	2.818E-05	22.4	5.050E-07	22.4
1215.0-1315.0	0.0	100.0	0.0	100.0
1315.0-1415.0	0.0	100.0	0.0	100.0
1415.0-1515.0	0.0	100.0	0.0	100.0
1515.0-1615.0	2.874E-04	7.5	6.584E-06	7.5
1615.0-1715.0	0.0	100.0	0.0	100.0
1715.0-1815.0	0.0	100.0	0.0	100.0
1815.0-1915.0	0.0	100.0	0.0	100.0
1915.0-2015.0	0.0	100.0	0.0	100.0
2015.0-2115.0	0.0	100.0	0.0	100.0
2115.0-2215.0	0.0	100.0	0.0	100.0
2215.0-2315.0	0.0	100.0	0.0	100.0
2315.0-2415.0	0.0	100.0	0.0	100.0
2415.0-2515.0	0.0	100.0	0.0	100.0
2515.0-2615.0	1.009E-03	4.5	3.225E-05	4.5

ANGLE TO +Z: (DEG)	DIFFER. FLUX: (1/CM2/S/STR)	C.V (%)	DIFFER. DOSE: (MICRO-GY/H/STR)	C.V (%)
0.0- 22.5	0.0	100.0	0.0	100.0
22.5- 45.0	0.0	100.0	0.0	100.0
45.0- 67.5	0.0	100.0	0.0	100.0
67.5- 90.0	0.0	100.0	0.0	100.0
90.0- 112.5	5.909E-02	2.6	1.006E-03	4.0
112.5- 135.0	6.762E-02	2.7	1.106E-03	4.1
135.0- 157.5	6.276E-02	3.8	1.084E-03	5.5
157.5- 180.0	5.905E-02	6.8	9.408E-04	9.7

RUNNING TIME: 19.2 SEC.

SOURCE: IDENT.NO. 2 TYPE: RA-CHAIN UNCOLLIDED PART NUMBER OF SIMULATIONS: 2200

FLUX: 3.392E-01 (1/CM2/S) (0.8%) AVERAGE ENERGY: 1021.7 KEV (1.4%) DOSE RATE: 5.181E-03 (MICRO-GY/H) (1.9%)

RESPONSE OF THE G-M/AL DETECTOR: 1.217E-01 CPS (2.1%)

RESPONSE OF THE CASO/AL2 DETECTOR: 5.375E-03 REL.TL (1.8%)

DIFFERENTIAL SPECTRA:

ENERGY: (KEV)	DIFFER. FLUX: (1/CM2/S/KEV)	C.V (%)	DIFFER. DOSE: (MICRO-GY/H/KEV)	C.V (%)
15.0- 115.0	1.623E-05	14.0	1.886E-08	13.9
115.0- 215.0	2.762E-05	17.6	7.813E-08	17.6
215.0- 315.0	2.912E-04	5.5	1.338E-06	5.6
315.0- 415.0	4.456E-04	4.5	2.657E-06	4.5
415.0- 515.0	1.948E-05	25.1	1.592E-07	25.1
515.0- 615.0	7.358E-04	3.8	7.628E-06	3.8
615.0- 715.0	3.310E-05	21.2	3.809E-07	21.2
715.0- 815.0	8.879E-05	13.2	1.143E-06	13.2
815.0- 915.0	4.011E-05	19.9	5.426E-07	19.9
915.0-1015.0	5.829E-05	17.1	8.859E-07	17.1
1015.0-1115.0	0.0	100.0	0.0	100.0
1115.0-1215.0	3.535E-04	7.0	6.230E-06	7.0
1215.0-1315.0	1.598E-04	11.0	3.055E-06	11.0
1315.0-1415.0	2.252E-04	9.5	4.688E-06	9.5
1415.0-1515.0	0.0	100.0	0.0	100.0
1515.0-1615.0	8.877E-05	15.7	1.983E-06	15.7
1615.0-1715.0	4.669E-05	22.3	1.099E-06	22.3
1715.0-1815.0	4.514E-04	7.0	1.114E-05	7.0
1815.0-1915.0	7.677E-05	17.8	1.963E-06	17.8
1915.0-2015.0	0.0	100.0	0.0	100.0
2015.0-2115.0	0.0	100.0	0.0	100.0
2115.0-2215.0	1.789E-04	12.2	5.114E-06	12.2
2215.0-2315.0	0.0	100.0	0.0	100.0
2315.0-2415.0	0.0	100.0	0.0	100.0
2415.0-2515.0	5.591E-05	22.8	1.717E-06	22.8
2515.0-2615.0	0.0	100.0	0.0	100.0

ANGLE TO +Z: (DEG)	DIFFER. FLUX: (1/CM2/S/STR)	C.V (%)	DIFFER. DOSE: (MICRO-GY/H/STR)	C.V (%)
0.0- 22.5	0.0	100.0	0.0	100.0
22.5- 45.0	0.0	100.0	0.0	100.0
45.0- 67.5	0.0	100.0	0.0	100.0
67.5- 90.0	0.0	100.0	0.0	100.0
90.0- 112.5	5.279E-02	3.0	8.160E-04	4.1
112.5- 135.0	5.699E-02	3.3	8.597E-04	4.5
135.0- 157.5	5.204E-02	4.6	8.084E-04	6.0
157.5- 180.0	5.296E-02	8.0	7.652E-04	10.7

RUNNING TIME: 12.5 SEC.

SOURCE: IDENT.NO. 3 TYPE: K-40 UNCOLLIDED PART NUMBER OF SIMULATIONS: 100

FLUX: 3.071E-01 (1/CM2/S) AVERAGE ENERGY: 1461.0 KEV DOSE RATE: 6.631E-03 (MICRO-GY/H)
(0.5%) (0.0%) (0.5%)

RESPONSE OF THE G-M/AL DETECTOR: 1.616E-01 CPS
(0.9%)
RESPONSE OF THE CASO/AL2 DETECTOR: 6.631E-03 REL.TL
(0.5%)

DIFFERENTIAL SPECTRA:

ENERGY: (KEV)	DIFFER. FLUX: (1/CM2/S/KEV)	C.V (%)	DIFFER. DOSE: (MICRO-GY/H/KEV)	C.V (%)
15.0- 115.0	0.0	100.0	0.0	100.0
115.0- 215.0	0.0	100.0	0.0	100.0
215.0- 315.0	0.0	100.0	0.0	100.0
315.0- 415.0	0.0	100.0	0.0	100.0
415.0- 515.0	0.0	100.0	0.0	100.0
515.0- 615.0	0.0	100.0	0.0	100.0
615.0- 715.0	0.0	100.0	0.0	100.0
715.0- 815.0	0.0	100.0	0.0	100.0
815.0- 915.0	0.0	100.0	0.0	100.0
915.0-1015.0	0.0	100.0	0.0	100.0
1015.0-1115.0	0.0	100.0	0.0	100.0
1115.0-1215.0	0.0	100.0	0.0	100.0
1215.0-1315.0	0.0	100.0	0.0	100.0
1315.0-1415.0	0.0	100.0	0.0	100.0
1415.0-1515.0	3.071E-03	0.5	6.631E-05	0.5
1515.0-1615.0	0.0	100.0	0.0	100.0
1615.0-1715.0	0.0	100.0	0.0	100.0
1715.0-1815.0	0.0	100.0	0.0	100.0
1815.0-1915.0	0.0	100.0	0.0	100.0
1915.0-2015.0	0.0	100.0	0.0	100.0
2015.0-2115.0	0.0	100.0	0.0	100.0
2115.0-2215.0	0.0	100.0	0.0	100.0
2215.0-2315.0	0.0	100.0	0.0	100.0
2315.0-2415.0	0.0	100.0	0.0	100.0
2415.0-2515.0	0.0	100.0	0.0	100.0
2515.0-2615.0	0.0	100.0	0.0	100.0

ANGLE TO +Z: (DEG)	DIFFER. FLUX: (1/CM2/S/STR)	C.V (%)	DIFFER. DOSE: (MICRO-GY/H/STR)	C.V (%)
0.0- 22.5	0.0	100.0	0.0	100.0
22.5- 45.0	0.0	100.0	0.0	100.0
45.0- 67.5	0.0	100.0	0.0	100.0
67.5- 90.0	0.0	100.0	0.0	100.0
90.0- 112.5	4.546E-02	13.1	9.814E-04	13.1
112.5- 135.0	5.537E-02	13.3	1.195E-03	13.3
135.0- 157.5	4.851E-02	19.4	1.047E-03	19.4
157.5- 180.0	3.953E-02	39.6	8.534E-04	39.6

RUNNING TIME: 0.0 SEC.

SOURCE: IDENT.NO. 4 TYPE: CS-137 UNCOLLIDED PART NUMBER OF SIMULATIONS: 300

FLUX: 4.525E-02 (1/CM2/S) AVERAGE ENERGY: 661.6 KEV DOSE RATE: 5.066E-04 (MICRO-GY/H)
(1.8%) (0.0%) (1.9%)

RESPONSE OF THE G-M/AL DETECTOR: 1.041E-02 CPS
(1.7%)
RESPONSE OF THE CASO/AL2 DETECTOR: 5.119E-04 REL.TL
(1.9%)

DIFFERENTIAL SPECTRA:

ENERGY: (KEV)	DIFFER. FLUX: (1/CM2/S/KEV)	C.V (%)	DIFFER. DOSE: (MICRO-GY/H/KEV)	C.V (%)
15.0- 115.0	0.0	100.0	0.0	100.0
115.0- 215.0	0.0	100.0	0.0	100.0
215.0- 315.0	0.0	100.0	0.0	100.0
315.0- 415.0	0.0	100.0	0.0	100.0
415.0- 515.0	0.0	100.0	0.0	100.0
515.0- 615.0	0.0	100.0	0.0	100.0
615.0- 715.0	4.525E-04	1.8	5.066E-06	1.9
715.0- 815.0	0.0	100.0	0.0	100.0
815.0- 915.0	0.0	100.0	0.0	100.0
915.0-1015.0	0.0	100.0	0.0	100.0
1015.0-1115.0	0.0	100.0	0.0	100.0
1115.0-1215.0	0.0	100.0	0.0	100.0
1215.0-1315.0	0.0	100.0	0.0	100.0
1315.0-1415.0	0.0	100.0	0.0	100.0
1415.0-1515.0	0.0	100.0	0.0	100.0
1515.0-1615.0	0.0	100.0	0.0	100.0
1615.0-1715.0	0.0	100.0	0.0	100.0
1715.0-1815.0	0.0	100.0	0.0	100.0
1815.0-1915.0	0.0	100.0	0.0	100.0
1915.0-2015.0	0.0	100.0	0.0	100.0
2015.0-2115.0	0.0	100.0	0.0	100.0
2115.0-2215.0	0.0	100.0	0.0	100.0
2215.0-2315.0	0.0	100.0	0.0	100.0
2315.0-2415.0	0.0	100.0	0.0	100.0
2415.0-2515.0	0.0	100.0	0.0	100.0
2515.0-2615.0	0.0	100.0	0.0	100.0

ANGLE TO +Z: (DEG)	DIFFER. FLUX: (1/CM2/S/STR)	C.V (%)	DIFFER. DOSE: (MICRO-GY/H/STR)	C.V (%)
0.0- 22.5	0.0	100.0	0.0	100.0
22.5- 45.0	0.0	100.0	0.0	100.0
45.0- 67.5	0.0	100.0	0.0	100.0
67.5- 90.0	0.0	100.0	0.0	100.0
90.0- 112.5	9.193E-03	7.9	1.029E-04	7.9
112.5- 135.0	6.826E-03	8.0	7.642E-05	8.0
135.0- 157.5	5.174E-03	10.9	5.793E-05	10.9
157.5- 180.0	4.562E-03	20.0	5.108E-05	20.0

RUNNING TIME: 1.3 SEC.

SOURCE: IDENT.NO. 1 TYPE: TH-CHAIN SCATTERED PART NUMBER OF SIMULATIONS:10000

FLUX: 1.763E 00 (1/CM2/S) AVERAGE ENERGY: 250.6 KEV DOSE RATE: 6.903E-03 (MICRO-GY/H)
(4.1%) (2.9%) (1.8%)

RESPONSE OF THE G-M/AL DETECTOR: 1.974E-01 CPS
(2.4%)

RESPONSE OF THE CASO/AL2 DETECTOR: 1.273E-02 REL.TL
(3.6%)

DIFFERENTIAL SPECTRA;

ENERGY: (KEV)	DIFFER. FLUX: (1/CM2/S/KEV)	C.V (%)	DIFFER. DOSE: (MICRO-GY/H/KEV)	C.V (%)
15.0- 115.0	7.687E-03	8.4	9.069E-06	8.2
115.0- 215.0	4.552E-03	7.3	1.035E-05	6.9
215.0- 315.0	1.773E-03	7.3	7.291E-06	7.2
315.0- 415.0	9.858E-04	6.9	6.017E-06	6.8
415.0- 515.0	6.639E-04	6.9	5.233E-06	6.9
515.0- 615.0	4.360E-04	7.2	4.163E-06	7.1
615.0- 715.0	2.853E-04	7.3	3.198E-06	7.3
715.0- 815.0	2.697E-04	7.0	3.430E-06	6.9
815.0- 915.0	2.008E-04	6.9	2.847E-06	6.9
915.0-1015.0	1.045E-04	7.1	1.622E-06	7.1
1015.0-1115.0	7.520E-05	6.8	1.269E-06	6.8
1115.0-1215.0	6.216E-05	7.1	1.126E-06	7.1
1215.0-1315.0	5.970E-05	7.1	1.155E-06	7.1
1315.0-1415.0	5.270E-05	7.3	1.082E-06	7.3
1415.0-1515.0	5.644E-05	7.0	1.221E-06	7.0
1515.0-1615.0	4.767E-05	7.1	1.080E-06	7.1
1615.0-1715.0	3.306E-05	7.6	7.845E-07	7.6
1715.0-1815.0	2.965E-05	7.7	7.327E-07	7.7
1815.0-1915.0	3.391E-05	7.0	8.721E-07	7.0
1915.0-2015.0	3.531E-05	7.0	9.402E-07	7.0
2015.0-2115.0	3.098E-05	7.3	8.534E-07	7.3
2115.0-2215.0	3.438E-05	7.0	9.747E-07	7.0
2215.0-2315.0	3.252E-05	7.1	9.503E-07	7.1
2315.0-2415.0	2.973E-05	7.3	8.931E-07	7.3
2415.0-2515.0	3.097E-05	7.2	9.558E-07	7.2
2515.0-2615.0	3.006E-05	7.2	9.493E-07	7.2

ANGLE TO +Z: (DEG)	DIFFER. FLUX: (1/CM2/S/STR)	C.V (%)	DIFFER. DOSE: (MICRO-GY/H/STR)	C.V (%)
0.0- 22.5	1.164E-01	30.7	1.778E-04	24.9
22.5- 45.0	9.516E-02	20.2	1.864E-04	15.3
45.0- 67.5	1.302E-01	14.8	2.469E-04	9.9
67.5- 90.0	1.082E-01	11.1	3.275E-04	5.6
90.0- 112.5	1.645E-01	7.7	7.636E-04	3.4
112.5- 135.0	1.617E-01	7.4	8.509E-04	3.6
135.0- 157.5	1.803E-01	9.4	9.340E-04	4.7
157.5- 180.0	1.709E-01	15.2	9.043E-04	8.0

RUNNING TIME: 1140.0 SEC.

SOURCE: IDENT.NO. 2 TYPE: RA-CHAIN SCATTERED PART NUMBER OF SIMULATIONS:10000

FLUX: 1.568E 00 (1/CM2/S) AVERAGE ENERGY: 236.6 KEV DOSE RATE: 5.903E-03 (MICRO-GY/H)
(4.1%) (2.8%) (1.9%)

RESPONSE OF THE G-M/AL DETECTOR: 1.700E-01 CPS
(2.6%)
RESPONSE OF THE CASO/AL2 DETECTOR: 1.101E-02 REL.TL
(3.6%)

DIFFERENTIAL SPECTRA:

ENERGY: (KEV)	DIFFER. FLUX: (1/CM2/S/KEV)	C.V (%)	DIFFER. DOSE: (MICRO-GY/H/KEV)	C.V (%)
15.0- 115.0	6.631E-03	8.4	7.823E-06	8.1
115.0- 215.0	4.082E-03	7.5	9.273E-06	7.1
215.0- 315.0	1.802E-03	7.3	7.454E-06	7.2
315.0- 415.0	9.317E-04	7.1	5.648E-06	7.0
415.0- 515.0	5.796E-04	7.0	4.564E-06	7.0
515.0- 615.0	4.237E-04	7.2	4.055E-06	7.2
615.0- 715.0	2.001E-04	7.3	2.244E-06	7.3
715.0- 815.0	1.862E-04	7.1	2.368E-06	7.1
815.0- 915.0	1.469E-04	7.1	2.086E-06	7.1
915.0-1015.0	1.353E-04	7.1	2.109E-06	7.1
1015.0-1115.0	1.394E-04	6.7	2.355E-06	6.7
1115.0-1215.0	8.948E-05	7.0	1.619E-06	7.0
1215.0-1315.0	7.441E-05	7.1	1.437E-06	7.1
1315.0-1415.0	6.067E-05	7.2	1.244E-06	7.2
1415.0-1515.0	5.257E-05	7.0	1.137E-06	7.0
1515.0-1615.0	4.554E-05	6.9	1.033E-06	6.9
1615.0-1715.0	3.907E-05	7.2	9.264E-07	7.2
1715.0-1815.0	2.192E-05	8.4	5.388E-07	8.4
1815.0-1915.0	1.090E-05	7.0	2.799E-07	7.0
1915.0-2015.0	1.006E-05	6.8	2.678E-07	6.8
2015.0-2115.0	8.968E-06	7.1	2.471E-07	7.1
2115.0-2215.0	8.123E-06	6.9	2.302E-07	6.9
2215.0-2315.0	1.687E-06	7.0	4.928E-08	7.0
2315.0-2415.0	1.535E-06	7.3	4.611E-08	7.3
2415.0-2515.0	4.105E-07	14.3	1.255E-08	14.3
2515.0-2615.0	0.0	100.0	0.0	100.0

ANGLE TO +Z: (DEG)	DIFFER. FLUX: (1/CM2/S/STR)	C.V (%)	DIFFER. DOSE: (MICRO-GY/H/STR)	C.V (%)
0.0- 22.5	9.328E-02	30.1	1.488E-04	24.2
22.5- 45.0	8.267E-02	20.7	1.667E-04	16.0
45.0- 67.5	1.143E-01	14.2	2.165E-04	9.7
67.5- 90.0	9.861E-02	11.3	2.860E-04	5.9
90.0- 112.5	1.458E-01	7.8	6.291E-04	3.8
112.5- 135.0	1.458E-01	7.5	7.341E-04	3.9
135.0- 157.5	1.634E-01	9.2	8.020E-04	5.2
157.5- 180.0	1.476E-01	14.3	7.847E-04	8.2

RUNNING TIME: 1140.0 SEC.

SOURCE: IDENT.NO. 3 TYPE: K-40 SCATTERED PART NUMBER OF SIMULATIONS:10000

FLUX: 1.263E 00 (1/CM2/S) AVERAGE ENERGY: 322.7 KEV DOSE RATE: 6.528E-03 (MICRO-GY/H)
(3.9%) (3.1%) (1.8%)

RESPONSE OF THE G-M/AL DETECTOR: 1.727E-01 CPS
(2.2%)
RESPONSE OF THE CASO/AL2 DETECTOR: 1.015E-02 REL.TL
(3.2%)

DIFFERENTIAL SPECTRA:

ENERGY: (KEV)	DIFFER. FLUX: (1/CM2/S/KEV)	C.V (%)	DIFFER. DOSE: (MICRO-GY/H/KEV)	C.V (%)
15.0- 115.0	4.565E-03	9.5	5.368E-06	9.3
115.0- 215.0	2.702E-03	8.2	6.173E-06	7.8
215.0- 315.0	1.393E-03	8.1	5.727E-06	7.9
315.0- 415.0	8.639E-04	7.6	5.272E-06	7.5
415.0- 515.0	5.493E-04	7.5	4.331E-06	7.5
515.0- 615.0	3.947E-04	7.7	3.784E-06	7.6
615.0- 715.0	3.019E-04	7.9	3.389E-06	8.0
715.0- 815.0	3.100E-04	7.5	3.947E-06	7.5
815.0- 915.0	2.450E-04	7.7	3.480E-06	7.6
915.0-1015.0	2.593E-04	7.5	4.044E-06	7.5
1015.0-1115.0	2.559E-04	7.2	4.326E-06	7.2
1115.0-1215.0	2.256E-04	7.3	4.088E-06	7.3
1215.0-1315.0	2.332E-04	7.3	4.510E-06	7.3
1315.0-1415.0	2.184E-04	7.2	4.482E-06	7.2
1415.0-1515.0	1.113E-04	10.0	2.374E-06	10.0
1515.0-1615.0	0.0	100.0	0.0	100.0
1615.0-1715.0	0.0	100.0	0.0	100.0
1715.0-1815.0	0.0	100.0	0.0	100.0
1815.0-1915.0	0.0	100.0	0.0	100.0
1915.0-2015.0	0.0	100.0	0.0	100.0
2015.0-2115.0	0.0	100.0	0.0	100.0
2115.0-2215.0	0.0	100.0	0.0	100.0
2215.0-2315.0	0.0	100.0	0.0	100.0
2315.0-2415.0	0.0	100.0	0.0	100.0
2415.0-2515.0	0.0	100.0	0.0	100.0
2515.0-2615.0	0.0	100.0	0.0	100.0

ANGLE TO +Z: (DEG)	DIFFER. FLUX: (1/CM2/S/STR)	C.V (%)	DIFFER. DOSE: (MICRO-GY/H/STR)	C.V (%)
0.0- 22.5	7.102E-02	31.7	1.215E-04	24.5
22.5- 45.0	7.577E-02	20.8	1.652E-04	14.6
45.0- 67.5	8.777E-02	14.1	2.008E-04	9.3
67.5- 90.0	7.836E-02	11.2	2.962E-04	5.7
90.0- 112.5	1.151E-01	7.3	7.105E-04	3.7
112.5- 135.0	1.211E-01	7.0	8.500E-04	3.8
135.0- 157.5	1.324E-01	8.1	9.123E-04	4.9
157.5- 180.0	1.135E-01	11.5	9.222E-04	7.6

RUNNING TIME: 1140.0 SEC.

SOURCE: IDENT.NO. 4 TYPE: CS-137 SCATTERED PART NUMBER OF SIMULATIONS:10000

FLUX: 1.175E-01 (1/CM2/S) AVERAGE ENERGY: 205.1 KEV DOSE RATE: 3.905E-04 (MICRO-GY/H)
(4.6%) (2.9%) (3.3%)

RESPONSE OF THE G-M/AL DETECTOR: 1.121E-02 CPS
(3.7%)

RESPONSE OF THE CASO/AL2 DETECTOR: 7.610E-04 REL.TL
(4.4%)

DIFFERENTIAL SPECTRA:

ENERGY: (KEV)	DIFFER. FLUX: (1/CM2/S/KEV)	C.V (%)	DIFFER. DOSE: (MICRO-GY/H/KEV)	C.V (%)
15.0- 115.0	4.622E-04	9.9	5.497E-07	9.8
115.0- 215.0	3.154E-04	8.0	7.394E-07	7.8
215.0- 315.0	1.544E-04	8.9	6.434E-07	8.9
315.0- 415.0	8.377E-05	8.0	5.150E-07	8.0
415.0- 515.0	6.513E-05	8.7	5.135E-07	8.6
515.0- 615.0	6.626E-05	9.0	6.399E-07	9.0
615.0- 715.0	2.816E-05	13.8	3.046E-07	13.8
715.0- 815.0	0.0	100.0	0.0	100.0
815.0- 915.0	0.0	100.0	0.0	100.0
915.0-1015.0	0.0	100.0	0.0	100.0
1015.0-1115.0	0.0	100.0	0.0	100.0
1115.0-1215.0	0.0	100.0	0.0	100.0
1215.0-1315.0	0.0	100.0	0.0	100.0
1315.0-1415.0	0.0	100.0	0.0	100.0
1415.0-1515.0	0.0	100.0	0.0	100.0
1515.0-1615.0	0.0	100.0	0.0	100.0
1615.0-1715.0	0.0	100.0	0.0	100.0
1715.0-1815.0	0.0	100.0	0.0	100.0
1815.0-1915.0	0.0	100.0	0.0	100.0
1915.0-2015.0	0.0	100.0	0.0	100.0
2015.0-2115.0	0.0	100.0	0.0	100.0
2115.0-2215.0	0.0	100.0	0.0	100.0
2215.0-2315.0	0.0	100.0	0.0	100.0
2315.0-2415.0	0.0	100.0	0.0	100.0
2415.0-2515.0	0.0	100.0	0.0	100.0
2515.0-2615.0	0.0	100.0	0.0	100.0

ANGLE TO +Z: (DEG)	DIFFER. FLUX: (1/CM2/S/STR)	C.V (%)	DIFFER. DOSE: (MICRO-GY/H/STR)	C.V (%)
0.0- 22.5	7.431E-03	31.1	1.189E-05	26.0
22.5- 45.0	6.445E-03	21.0	1.351E-05	15.3
45.0- 67.5	9.122E-03	14.4	1.850E-05	10.7
67.5- 90.0	7.532E-03	9.9	2.793E-05	8.3
90.0- 112.5	1.220E-02	8.5	5.279E-05	6.5
112.5- 135.0	1.054E-02	10.5	3.844E-05	7.3
135.0- 157.5	9.687E-03	12.2	3.183E-05	9.2
157.5- 180.0	9.373E-03	30.3	2.713E-05	21.7

RUNNING TIME: 1140.0 SEC.

SOURCE: IDENT.NO. 1 TYPE: TH-CHAIN

TOTAL VALUES

FLUX: 2.156E 00 (1/CM2/S)
(3.4%)

AVERAGE ENERGY: 424.8 KEV
(2.9%)

DOSE RATE: 1.350E-02 (MICRO-GY/H)
(1.3%)

RESPONSE OF THE G-M/AL DETECTOR: 3.535E-01 CPS
(1.6%)

RESPONSE OF THE CASO/AL2 DETECTOR: 1.954E-02 REL.TL
(2.5%)

DIFFERENTIAL SPECTRA:

ENERGY: (KEV)	DIFFER. FLUX: (1/CM2/S/KEV)	C.V (%)	DIFFER. DOSE: (MICRO-GY/H/KEV)	C.V (%)
15.0- 115.0	7.712E-03	8.4	9.101E-06	8.2
115.0- 215.0	4.623E-03	7.2	1.054E-05	6.8
215.0- 315.0	2.303E-03	5.7	9.410E-06	5.6
315.0- 415.0	1.174E-03	5.9	7.111E-06	5.8
415.0- 515.0	8.396E-04	5.6	6.718E-06	5.6
515.0- 615.0	8.500E-04	4.3	8.275E-06	4.3
615.0- 715.0	2.853E-04	7.3	3.198E-06	7.3
715.0- 815.0	4.995E-04	4.9	6.343E-06	4.9
815.0- 915.0	7.964E-04	3.7	1.158E-05	3.7
915.0-1015.0	4.871E-04	4.7	7.600E-06	4.7
1015.0-1115.0	7.520E-05	6.8	1.269E-06	6.8
1115.0-1215.0	9.034E-05	8.5	1.631E-06	8.5
1215.0-1315.0	5.970E-05	7.1	1.155E-06	7.1
1315.0-1415.0	5.270E-05	7.3	1.082E-06	7.3
1415.0-1515.0	5.644E-05	7.0	1.221E-06	7.0
1515.0-1615.0	3.351E-04	6.6	7.664E-06	6.6
1615.0-1715.0	3.306E-05	7.6	7.845E-07	7.6
1715.0-1815.0	2.965E-05	7.7	7.327E-07	7.7
1815.0-1915.0	3.391E-05	7.0	8.721E-07	7.0
1915.0-2015.0	3.531E-05	7.0	9.402E-07	7.0
2015.0-2115.0	3.098E-05	7.3	8.534E-07	7.3
2115.0-2215.0	3.438E-05	7.0	9.747E-07	7.0
2215.0-2315.0	3.252E-05	7.1	9.503E-07	7.1
2315.0-2415.0	2.973E-05	7.3	8.931E-07	7.3
2415.0-2515.0	3.097E-05	7.2	9.558E-07	7.2
2515.0-2615.0	1.039E-03	4.3	3.320E-05	4.3

ANGLE TO +Z: (DEG)	DIFFER. FLUX: (1/CM2/S/STR)	C.V (%)	DIFFER. DOSE: (MICRO-GY/H/STR)	C.V (%)
0.0- 22.5	1.164E-01	30.7	1.778E-04	24.9
22.5- 45.0	9.516E-02	20.2	1.864E-04	15.3
45.0- 67.5	1.302E-01	14.8	2.469E-04	9.9
67.5- 90.0	1.082E-01	11.1	3.275E-04	5.6
90.0- 112.5	2.236E-01	5.7	1.769E-03	2.7
112.5- 135.0	2.293E-01	5.3	1.957E-03	2.8
135.0- 157.5	2.430E-01	7.0	2.018E-03	3.7
157.5- 180.0	2.299E-01	11.4	1.845E-03	6.3

RUNNING TIME: 1159.3 SEC.

SOURCE: IDENT.NO. 2 TYPE: RA-CHAIN TOTAL VALUES

FLUX: 1,907E 00 (1/CM2/S) AVERAGE ENERGY: 376,3 KEV DOSE RATE: 1,108E-02 (MICRO-GY/H)
(3,4%) (2,8%) (1,4%)

RESPONSE OF THE G-M/AL DETECTOR: 2,917E-01 CPS
(1,7%)
RESPONSE OF THE CASO/AL2 DETECTOR: 1,639E-02 REL,TL
(2,5%)

DIFFERENTIAL SPECTRA;

ENERGY: (KEV)	DIFFER, FLUX: (1/CM2/S/KEV)	C,V (%)	DIFFER, DOSE: (MICRO-GY/H/KEV)	C,V (%)
15,0- 115,0	6,647E-03	8,3	7,842E-06	8,1
115,0- 215,0	4,109E-03	7,5	9,351E-06	7,0
215,0- 315,0	2,093E-03	6,3	8,792E-06	6,1
315,0- 415,0	1,377E-03	5,0	8,305E-06	5,0
415,0- 515,0	5,991E-04	6,8	4,723E-06	6,8
515,0- 615,0	1,159E-03	3,6	1,168E-05	3,5
615,0- 715,0	2,332E-04	7,0	2,625E-06	7,0
715,0- 815,0	2,750E-04	6,4	3,511E-06	6,4
815,0- 915,0	1,870E-04	7,0	2,629E-06	7,0
915,0-1015,0	1,936E-04	7,1	2,995E-06	7,1
1015,0-1115,0	1,394E-04	6,7	2,355E-06	6,7
1115,0-1215,0	4,430E-04	5,8	7,850E-06	5,8
1215,0-1315,0	2,342E-04	7,8	4,493E-06	7,8
1315,0-1415,0	2,859E-04	7,6	5,932E-06	7,6
1415,0-1515,0	5,257E-05	7,0	1,137E-06	7,0
1515,0-1615,0	1,343E-04	10,6	3,015E-06	10,6
1615,0-1715,0	8,575E-05	12,6	2,025E-06	12,5
1715,0-1815,0	4,734E-04	6,7	1,168E-05	6,7
1815,0-1915,0	8,768E-05	15,6	2,242E-06	15,6
1915,0-2015,0	1,006E-05	6,8	2,678E-07	6,8
2015,0-2115,0	8,968E-06	7,1	2,471E-07	7,1
2115,0-2215,0	1,870E-04	11,7	5,344E-06	11,7
2215,0-2315,0	1,687E-06	7,0	4,928E-08	7,0
2315,0-2415,0	1,535E-06	7,3	4,611E-08	7,3
2415,0-2515,0	5,632E-05	22,7	1,729E-06	22,7
2515,0-2615,0	0,0	100,0	0,0	100,0

ANGLE TO +Z: (DEG)	DIFFER, FLUX: (1/CM2/S/STR)	C,V (%)	DIFFER, DOSE: (MICRO-GY/H/STR)	C,V (%)
0,0- 22,5	9,328E-02	30,1	1,488E-04	24,2
22,5- 45,0	8,267E-02	20,7	1,667E-04	16,0
45,0- 67,5	1,143E-01	14,2	2,165E-04	9,7
67,5- 90,0	9,861E-02	11,3	2,860E-04	5,9
90,0- 112,5	1,986E-01	5,8	1,445E-03	2,9
112,5- 135,0	2,028E-01	5,5	1,594E-03	3,0
135,0- 157,5	2,154E-01	7,1	1,610E-03	4,0
157,5- 180,0	2,005E-01	10,7	1,550E-03	6,7

RUNNING TIME: 1152,5 SEC,

SOURCE: IDENT.NO. 3 TYPE: K-40 TOTAL VALUES

FLUX: 1.570E 00 (1/CM2/S) AVERAGE ENERGY: 545.4 KEV DOSE RATE: 1.316E-02 (MICRO-GY/H)
(3.2%) (2.7%) (0.9%)

RESPONSE OF THE G-M/AL DETECTOR: 3.343E-01 CPS
(1.2%)
RESPONSE OF THE CASO/AL2 DETECTOR: 1.678E-02 REL.TL
(1.9%)

DIFFERENTIAL SPECTRA:

ENERGY: (KEV)	DIFFER. FLUX: (1/CM2/S/KEV)	C.V (%)	DIFFER. DOSE: (MICRO-GY/H/KEV)	C.V (%)
15.0- 115.0	4.565E-03	9.5	5.368E-06	9.3
115.0- 215.0	2.702E-03	8.2	6.173E-06	7.8
215.0- 315.0	1.393E-03	8.1	5.727E-06	7.9
315.0- 415.0	8.639E-04	7.6	5.272E-06	7.5
415.0- 515.0	5.493E-04	7.5	4.331E-06	7.5
515.0- 615.0	3.947E-04	7.7	3.784E-06	7.6
615.0- 715.0	3.019E-04	7.9	3.389E-06	8.0
715.0- 815.0	3.100E-04	7.5	3.947E-06	7.5
815.0- 915.0	2.450E-04	7.7	3.480E-06	7.6
915.0-1015.0	2.593E-04	7.5	4.044E-06	7.5
1015.0-1115.0	2.559E-04	7.2	4.326E-06	7.2
1115.0-1215.0	2.256E-04	7.3	4.088E-06	7.3
1215.0-1315.0	2.332E-04	7.3	4.510E-06	7.3
1315.0-1415.0	2.184E-04	7.2	4.482E-06	7.2
1415.0-1515.0	3.183E-03	0.6	6.869E-05	0.6
1515.0-1615.0	0.0	100.0	0.0	100.0
1615.0-1715.0	0.0	100.0	0.0	100.0
1715.0-1815.0	0.0	100.0	0.0	100.0
1815.0-1915.0	0.0	100.0	0.0	100.0
1915.0-2015.0	0.0	100.0	0.0	100.0
2015.0-2115.0	0.0	100.0	0.0	100.0
2115.0-2215.0	0.0	100.0	0.0	100.0
2215.0-2315.0	0.0	100.0	0.0	100.0
2315.0-2415.0	0.0	100.0	0.0	100.0
2415.0-2515.0	0.0	100.0	0.0	100.0
2515.0-2615.0	0.0	100.0	0.0	100.0

ANGLE TO +Z: (DEG)	DIFFER. FLUX: (1/CM2/S/STR)	C.V (%)	DIFFER. DOSE: (MICRO-GY/H/STR)	C.V (%)
0.0- 22.5	7.102E-02	31.7	1.215E-04	24.5
22.5- 45.0	7.577E-02	20.8	1.652E-04	14.6
45.0- 67.5	8.777E-02	14.1	2.008E-04	9.3
67.5- 90.0	7.836E-02	11.2	2.902E-04	5.7
90.0- 112.5	1.606E-01	6.4	1.692E-03	7.8
112.5- 135.0	1.765E-01	6.3	2.045E-03	8.0
135.0- 157.5	1.809E-01	7.9	1.900E-03	10.6
157.5- 180.0	1.530E-01	13.3	1.776E-03	19.4

RUNNING TIME: 1140.0 SEC.

SOURCE: IDENT.NO. 4 TYPE: CS-137 TOTAL VALUES

FLUX: 1,628E-01 (1/CM2/S) AVERAGE ENERGY: 332,0 KEV DOSE RATE: 8,971E-04 (MICRO-GY/H)
(3,4%) (2,4%) (1,8%)

RESPONSE OF THE G-M/AL DETECTOR: 2,162E-02 CPS
(2,1%)
RESPONSE OF THE CASO/AL2 DETECTOR: 1,273E-03 REL,TL
(2,7%)

DIFFERENTIAL SPECTRA:

ENERGY: (KEV)	DIFFER, FLUX: (1/CM2/S/KEV)	C,V (%)	DIFFER, DOSE: (MICRO-GY/H/KEV)	C,V (%)
15,0- 115,0	4,622E-04	9,9	5,497E-07	9,8
115,0- 215,0	3,154E-04	8,0	7,394E-07	7,8
215,0- 315,0	1,544E-04	8,9	6,434E-07	8,9
315,0- 415,0	8,377E-05	8,0	5,150E-07	8,0
415,0- 515,0	6,513E-05	8,7	5,135E-07	8,6
515,0- 615,0	6,626E-05	9,0	6,399E-07	9,0
615,0- 715,0	4,806E-04	1,9	5,371E-06	1,9
715,0- 815,0	0,0	100,0	0,0	100,0
815,0- 915,0	0,0	100,0	0,0	100,0
915,0-1015,0	0,0	100,0	0,0	100,0
1015,0-1115,0	0,0	100,0	0,0	100,0
1115,0-1215,0	0,0	100,0	0,0	100,0
1215,0-1315,0	0,0	100,0	0,0	100,0
1315,0-1415,0	0,0	100,0	0,0	100,0
1415,0-1515,0	0,0	100,0	0,0	100,0
1515,0-1615,0	0,0	100,0	0,0	100,0
1615,0-1715,0	0,0	100,0	0,0	100,0
1715,0-1815,0	0,0	100,0	0,0	100,0
1815,0-1915,0	0,0	100,0	0,0	100,0
1915,0-2015,0	0,0	100,0	0,0	100,0
2015,0-2115,0	0,0	100,0	0,0	100,0
2115,0-2215,0	0,0	100,0	0,0	100,0
2215,0-2315,0	0,0	100,0	0,0	100,0
2315,0-2415,0	0,0	100,0	0,0	100,0
2415,0-2515,0	0,0	100,0	0,0	100,0
2515,0-2615,0	0,0	100,0	0,0	100,0

ANGLE TO +Z: (DEG)	DIFFER, FLUX: (1/CM2/S/STR)	C,V (%)	DIFFER, DOSE: (MICRO-GY/H/STR)	C,V (%)
0,0- 22,5	7,431E-03	31,1	1,189E-05	26,0
22,5- 45,0	6,445E-03	21,0	1,351E-05	15,3
45,0- 67,5	9,122E-03	14,4	1,850E-05	10,7
67,5- 90,0	7,532E-03	9,9	2,793E-05	8,3
90,0- 112,5	2,139E-02	5,9	1,557E-04	5,7
112,5- 135,0	1,737E-02	7,1	1,149E-04	5,9
135,0- 157,5	1,486E-02	8,8	8,976E-05	7,8
157,5- 180,0	1,393E-02	21,4	7,821E-05	15,1

RUNNING TIME: 1141,4 SEC,

TOTAL SUMMARY

FLUX: 5,796E 00 (1/CM2/S)
(1,9%)
DOSE RATE: 3,864E-02 (MICRO-GY/H)
(0,7%)
RESPONSE OF THE G-M/AL DETECTOR: 1,001E 00 CPS
(0,9%)
RESPONSE OF THE CASO/AL2 DETECTOR: 1,055E 00 REL.TL
(0,9%)

DIFFERENTIAL SPECTRA:

ENERGY: (KEV)	DIFFER. FLUX: (1/CM2/S/KEV)	C.V (%)	DIFFER. DOSE: (MICRO-GY/H/KEV)	C.V (%)
15,0- 115,0	1,939E-02	4,9	2,286E-05	4,8
115,0- 215,0	1,175E-02	4,3	2,680E-05	4,0
215,0- 315,0	5,944E-03	3,7	2,457E-05	3,6
315,0- 415,0	3,499E-03	3,4	2,120E-05	3,3
415,0- 515,0	2,053E-03	3,7	1,629E-05	3,6
515,0- 615,0	2,470E-03	2,6	2,438E-05	2,5
615,0- 715,0	1,301E-03	2,8	1,458E-05	2,8
715,0- 815,0	1,084E-03	3,5	1,380E-05	3,5
815,0- 915,0	1,228E-03	3,0	1,769E-05	3,0
915,0-1015,0	9,400E-04	3,5	1,464E-05	3,5
1015,0-1115,0	4,705E-04	4,5	7,950E-06	4,5
1115,0-1215,0	7,590E-04	4,1	1,357E-05	4,1
1215,0-1315,0	5,270E-04	4,8	1,016E-05	4,8
1315,0-1415,0	5,570E-04	4,9	1,150E-05	4,9
1415,0-1515,0	3,292E-03	0,6	7,105E-05	0,6
1515,0-1615,0	4,694E-04	5,6	1,068E-05	5,6
1615,0-1715,0	1,188E-04	9,3	2,810E-06	9,3
1715,0-1815,0	5,030E-04	6,3	1,241E-05	6,3
1815,0-1915,0	1,216E-04	11,5	3,115E-06	11,4
1915,0-2015,0	4,537E-05	5,6	1,208E-06	5,6
2015,0-2115,0	3,995E-05	5,9	1,101E-06	5,9
2115,0-2215,0	2,214E-04	9,9	6,319E-06	10,0
2215,0-2315,0	3,421E-05	6,8	9,996E-07	6,8
2315,0-2415,0	3,127E-05	7,0	9,393E-07	7,0
2415,0-2515,0	8,729E-05	14,9	2,685E-06	14,8
2515,0-2615,0	1,039E-03	4,3	3,320E-05	4,3

ANGLE TO +Z: (DEG)	DIFFER. FLUX: (1/CM2/S/STR)	C.V (%)	DIFFER. DOSE: (MICRO-GY/H/STR)	C.V (%)
0,0- 22,5	2,881E-01	17,6	4,600E-04	14,0
22,5- 45,0	2,600E-01	11,6	5,318E-04	8,6
45,0- 67,5	3,414E-01	8,2	6,827E-04	5,5
67,5- 90,0	2,927E-01	6,3	9,376E-04	3,2
90,0- 112,5	6,041E-01	3,3	5,062E-03	2,9
112,5- 135,0	6,259E-01	3,2	5,711E-03	3,1
135,0- 157,5	6,542E-01	4,1	5,677E-03	4,1
157,5- 180,0	5,974E-01	6,6	5,249E-03	7,2

Kiadja a Központi Fizikai Kutató Intézet
Felelős kiadó: Gyimesi Zoltán
Szakmai lektor: Németh István
Nyelvi lektor: Harvey Shenker
Gépelte: Beron Péterné
Példányszám: 330 Törzsszám: 81-533
Készült a KFKI sokszorosító üzemében
Felelős vezető: Nagy Károly
Budapest, 1981. szeptember hó